PB88-247705

BIOMECHANICAL ANALYSIS OF PERSONAL CTS ATTRIBUTES

JOSEPH M. ROLECKI

April 21, 1978

This work has been partially supported by an educational NIOSH Training Grant, Number 2T01-OH00161-05, and also by funds provided by a private industry.

ACKNOWLEDGEMENTS

My thanks goes to all the people who have helped make this report possible. I especially thank Dr. Tom Armstrong for his guidance and knowledge in the planning and execution of the experimentation, and his advice during the writing of this report. I would also like to thank Mr. James Foulke for his technical assistance, Patricia Brooks for her long hours of editing, typing, and encouragement, Edith Baise for her editing of the final report copy, and Susanne Elward for illustrations.

ABSTRACT

Carpal Tunnel Syndrome is caused by compression of the median nerve in the carpal tunnel of the wrist. Increases in tunnel pressure or direct impingement of the finger flexor tendons may contribute to this compression. This paper investigates the contribution of wrist size to flexor tendon geometry and high force loads on the tendons. An investigation is also made to determine if several chosen wrist bone dimensions are indicative of CTS occurrence. The major findings of the report show that tendon geometry and force loadings on the tendons change with wrist thickness, and that the chosen wrist dimensions are not indicative of CTS occurrence.

TABLE OF CONTENTS

LIST OF FIGURES

LIST OF TABLES

I. INTRODUCTION

1.1 PURPOSE OF REPORT

It is the intention of this report to focus on Carpal Tunnel Syndrome (CTS) as an occupational injury related to the structural characteristics of the individual human wrist. The report contains two main areas of analysis. The first involves a cadaver study to determine the geometry of the finger flexor tendons as they pass through the carpal tunnel of the wrist. The purpose of this section is to show different tendon curvatures and force loadings along the tendons in the carpal tunnel for different wrist sizes. Large force loadings may be an indicator that small wrist structures are predisposed to tenosynovitis and Carpal Tunnel Syndrome.

The second section of the report is concerned with the bone structure of the wrist as seen in radiographs of CTS and normal populations. The purpose of this section is to discover a relationship between various bone sizes, especially those sizes which determine carpal tunnel dimensions, and the occurrence of CTS.

1.2 RATIONALE FOR REPORT

This paper is written in conjunction with a National Institute for Occupational Safety and Health (NIOSH) traineeship grant and as a part of a research project sponsored by NIOSH and a private local industry. The research was conducted at the Human Performance and Safety Laboratory in the Industrial and Operations Engineering Department at the University of Michigan in Ann Arbor, Michigan. A two part

study is in process at the laboratory in an attempt to determine the etiology of CTS in the occupational environment. One aspect of the project is a field study which seeks to determine the relationships between the activity of the worker and the occurrence of CTS. The second aspect of the study focuses on the anatomical characteristics of the human wrist that may indicate which populations of workers are more prone to CTS. It is the second objective with which this paper is concerned.

It is hoped that the personal attributes found in this paper will be a foundation for predictive models and guidelines to be used in the industrial workplace to avert the occurrence of CTS there.

II. BACKGROUND

2.1 THE WRIST: ANATOMICAL DESCRIPTION

The long finger flexor tendons of the human hand allow for the powerful grasping and pinching motions which are so essential to everyday life. The wonderful engineering of the hand puts the mechanical devices, which facilitate finger flexion and power grip, away from the fingers in the upper forearm. This facilitates the functioning of small local finger muscles which give the hand its amazing dexterity. The fingers are flexed mainly by two groups of muscles, the flexor digitorum superficialis (FDS) and flexor digitorum profundus (FDP), which are located on the dorsal side of the arm. The superficialis attaches to the proximal areas along the radius and ulna. From the muscle mass in the forearm, the muscles are attached to the fingers by the long finger flexor tendons. These pass along the distal ends of the radius and ulna, over the carpal bones to the metacarpals, where they branch to each digit. Each of the digits 2 through 5 receive two of the tendons, one FDS and one FDP. The profundus tendon attaches to the distal phalange while the superficialis tendon, passing over the profundus, branches at the proximal-phalangeal joint and attaches to the middle phalange (Figure 2-1).

The first digit receives only one long tendon from the profundus group and is called the flexor policus longus (FPL). The FPL attaches to the distal phalange of the thumb. Unlike digits 2 through 4, the first digit is aided by a powerful local muscle group

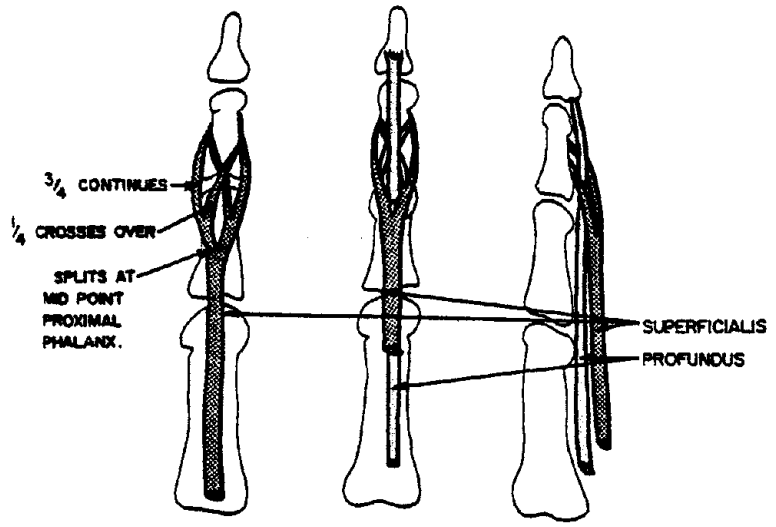

Figure 2-1: Tendon Attachment To Phalanges (Cailliet 1975)

which is located palmar to the first metacarpal called the thenar muscles. The thenar muscles are extremely important in such motions as pinching, grasping, pulling, and other motions which require strength in the opposing digit.

The flexor tendons are each encompassed by a thin sheath of synovium (Figure 2-2). The flexor synovium acts as a lubricating sleeve to allow smooth movement of the tendon between adjacent structures and over bounding structures of the wrist during extension and flexion.

The path of the flexor tendons from the point of the distal radius and ulna, over the carpal bones to the proximal ends of the metacarpals, is of special interest in this report; the tendons at this point pass through the structure of the carpal tunnel. The carpal tunnel is bounded on the dorsal side of the wrist by the two rows of carpal bones and on the palmar side by a tough ligament called the flexor retinaculum.

The carpal bones of the wrist are arranged in two rows; one distal row and one proximal row (Figure 2.3). The distal row consists of the hamate, capitate, pisiform, trapezoid, and trapezium bones. The proximal row consists of the triquetrum, lunate, and scaphoid bones. The pisiform of the distal row is a sesamoid bone which lies palmar to the hamate-triquetrum articulation.

The flexor retinaculum provides a less rigid palmar border of the carpal tunnel than the carpal bones. This band of fascia is divided into the palmar carpal ligament proximally and the transverse

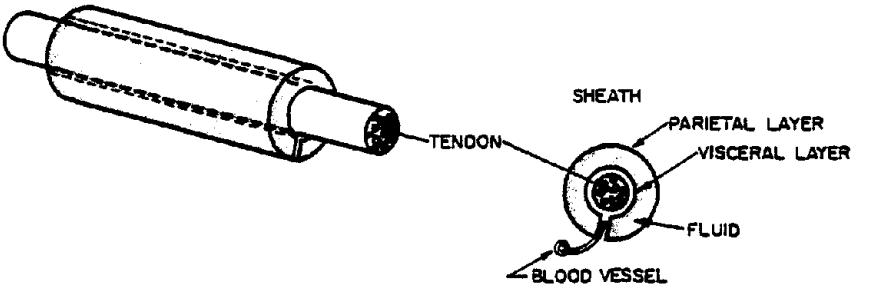

Figure 2-2: Flexor Tendon Sheaths (Cailliet, 1975)

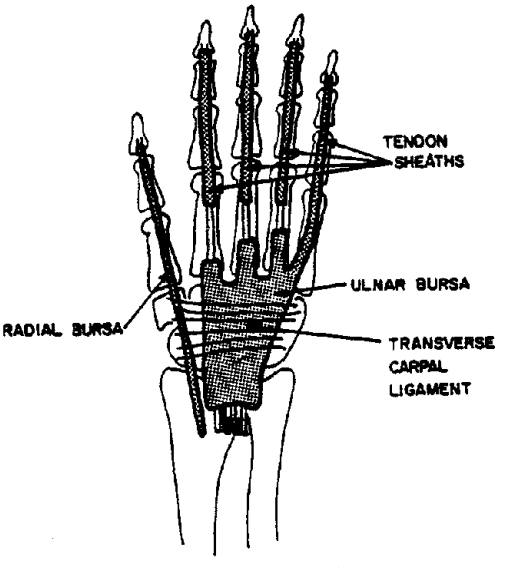

Figure 2-2: Flexor Tendon Sheaths (Cailliet, 1975- cont.)

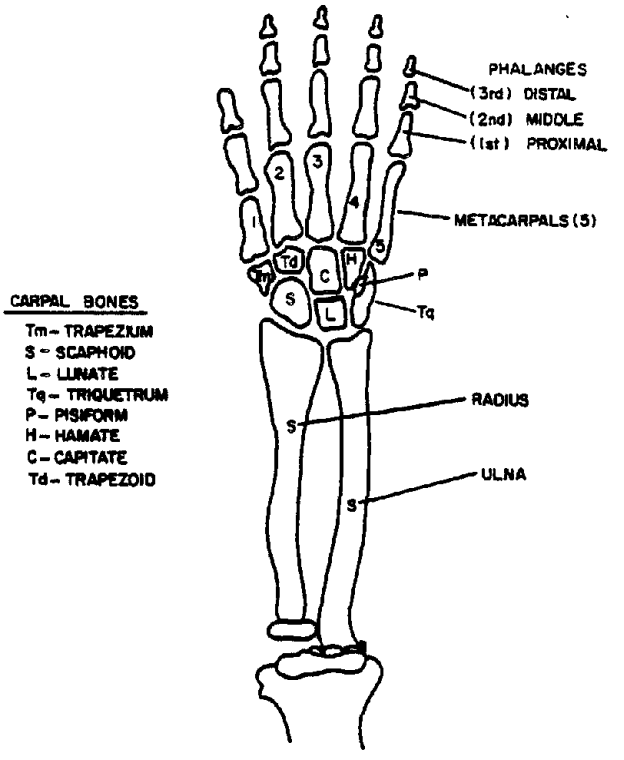

Figure 2-3: Bones of the Forearm, Hand, and Wrist (R.N. Gray, 1969)

carpal ligament distally. The palmar carpal ligament attaches laterally to the distal end of the ulna and medially to the radial styloid process. The ligament merges on its distal border with the transverse carpal ligament. The transverse carpal ligament attaches to the pisiform and hook of the hamate medially and to the tubercle of the trapezium and scaphoid laterally.

The carpal tunnel includes a major nerve, the median nerve, which innervates a large portion of the palmar side of the hand. The median nerve passes along the forearm between the flexor digitorum superficialis and profundus tendon groups. The nerve becomes superficial to both groups of tendons at the flexor retinaculum. In the distal portion of the carpal tunnel, the nerve

flattens and splits into three branches. These branches, the location of which have been shown to vary considerably (Ulrich, 1977), continue on to innervate muscles of the thenar eminence, the index and middle fingers, and the radial side of the ring finger (Figure 2-4).

A cross section of the carpal tunnel reveals the configuration of the flexor tendons and the median nerve as they pass through the carpal tunnel (Figure 2-5). The FPL lies most radial of the tendons and it has been proposed that the flexor tendons of the third and fourth digits lie directly beneath the median nerve (Smith, et al., 1977, Figure 2-6). When the wrist is flexed, the flexor tendons in the carpal tunnel impinge directly on the median nerve, pressing it against the flexor retinaculum. When the wrist is extended, large pressures are generated in the carpal tunnel. Brain (1947) has estimated that pressure within the carpal tunnel is increased three times over the pressure generated when the wrist is flexed (Figure 2-7). It has been proposed that this increased pressure leads to an ischemic median nerve when the hand is used in a strenuous manner (Sunderland, 1975).

2.2 THE WRIST: BIOMECHANICAL DESCRIPTION

When the wrist is flexed or extended, the finger flexor tendons pass against and around the bounding structures of the carpal tunnel. The tendons pass over the carpal bones during extension and over the flexor retinaculum during flexion (Armstrong and Chaffin, 1977).

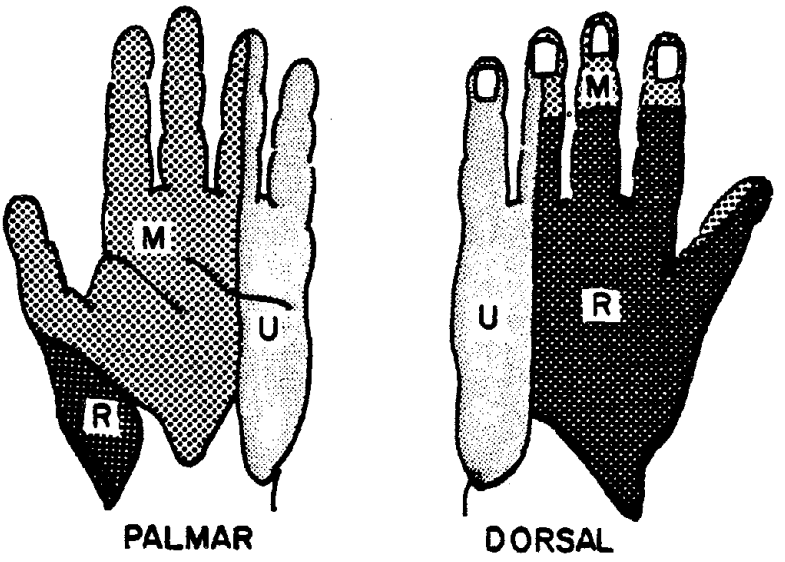

Figure 2-4: Areas of Innervation by the Median Nerve (Cailliet, 1975)

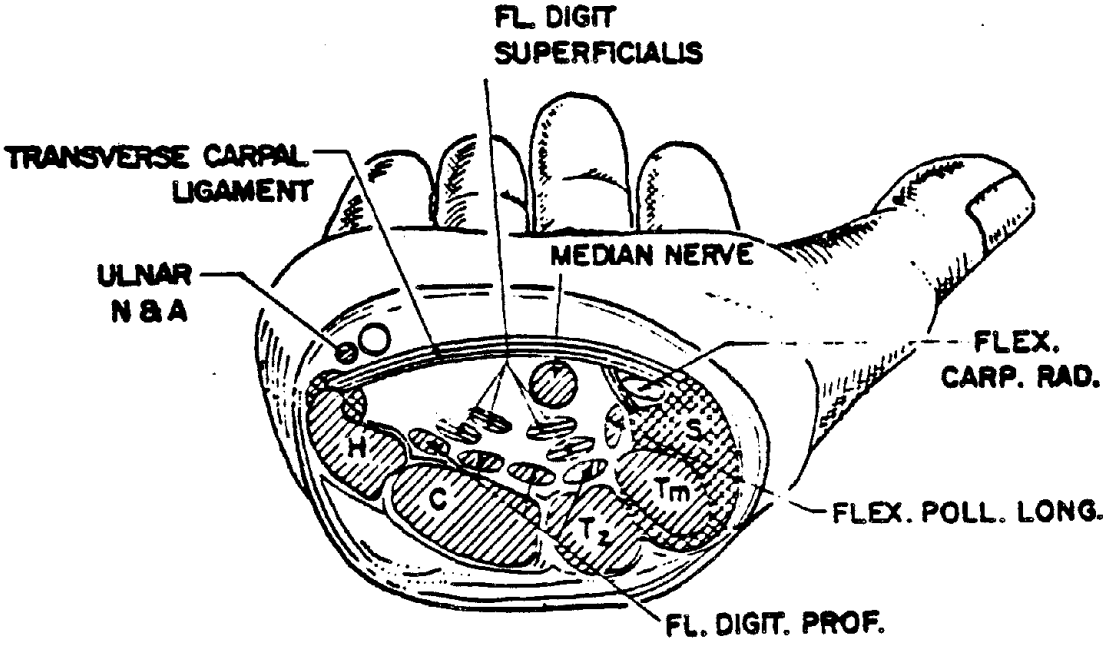

Figure 2-5: Contents of the Carpal Tunnel (adapted from Cailliet, 1975)

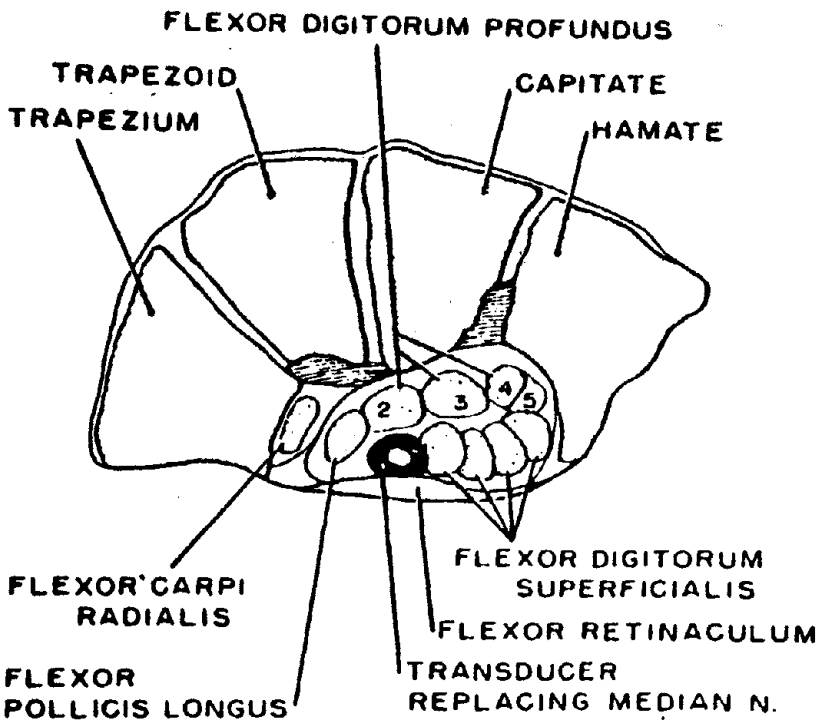

Fig 2—Relationship of median nerve and tendons in carpal tunnel (drawn from frozen section).

Figure 2-6: Cross-Sectional View of the Carpal Tunnel and Tendon Arrangement (Adapted from Smith, et al., 1977)

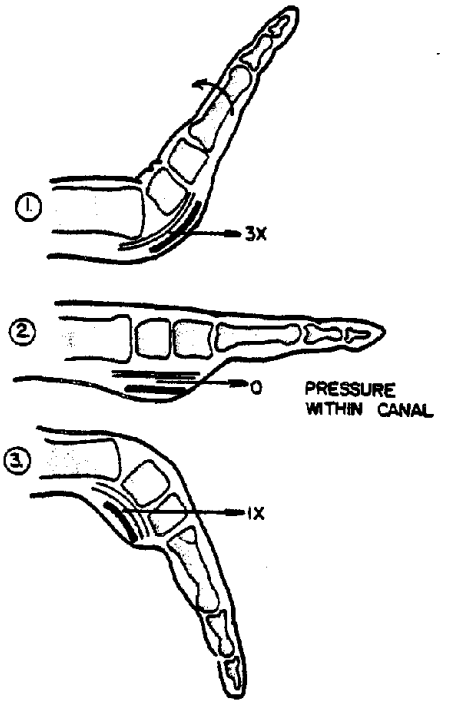

Figure 2-7: Carpal Tunnel Pressure Changes During Extension and Flexion (Cailliet 1975)

These structures may be described as trochlea (anatomical pulley) for the tendons during wrist extension and flexion.

With the wrist extended or flexed, the carpal bones or flexor retinaculum may be described as an arc of a pulley, and the tendons are loaded with forces similar to a rope over a pulley.

The load generated along the length of the tendon, which is against the carpal bones, is described by Leveau (1977) as:

$$\text{Load (force/arc length)} = \frac{F_t e^{u\theta}}{r} \qquad (2.1)$$

where:

F_t = tendon tension

θ = angle of wrist deviation

r = radius of the trochlea

The coefficient of friction (u) between the tendon and cartilage has been estimated to be about .02 (Leveau, 1977). At this small value the friction component of the load may be omitted. The expression for load then reduces to:

$$\text{Load (force/arc length)} = \frac{F_t}{r} \qquad (2.2)$$

This relationship shows that load will increase as joint thickness decreases. (Figure 2-8)

The resultant force exerted on the tendon by the trochlea is described by Leveau (1977) as:

$$F_r = 2F_t \left(\sin \left(\frac{\theta}{2}\right)\right) \qquad (2.3)$$

where:

F_r = resultant force on tendon

F_t = tendon tension

θ = angle of wrist deviation

This relationship shows that the resultant force on the tendon will increase as joint angle increases. (Figure 2-9)

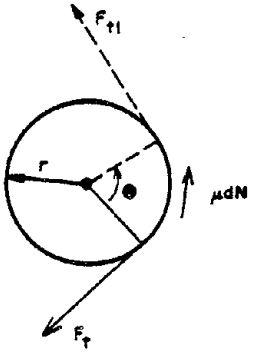

$$\text{LOAD} = \frac{F_t e^{\mu\theta}}{r}$$

WHERE: r = RADIUS OF PULLEY

θ = INCLUDED ANGLE OF THE AREA IN CONTACT.

μ = COEFFICIENT OF FRICTION.

F_{t1} & F_t = BELT TENSION

μdN = FORCE OF FRICTION.

Figure 2-8: Belt and Pulley - Free Body Design

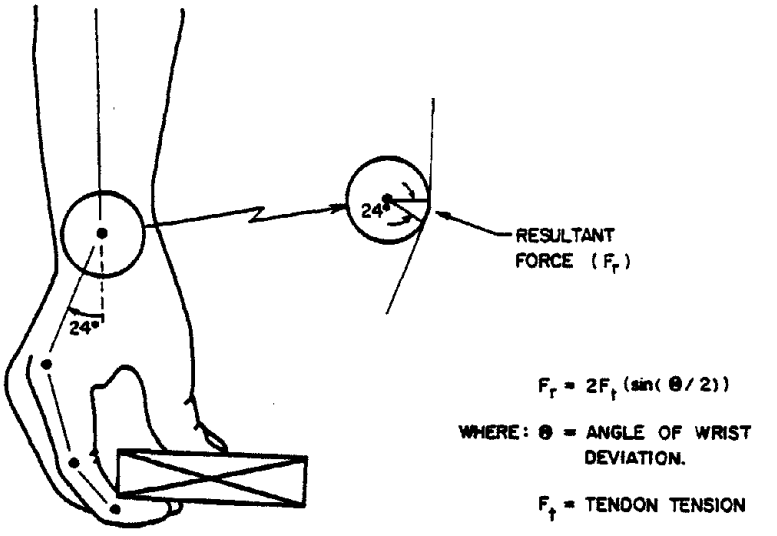

Figure 2-9: Area of Tendon Contact

By combining equations (2.2) and (2.3), the resultant force on the tendon may be described as a function of wrist thickness and wrist angle:

$$F_r = \frac{2 \text{ load}}{r} \quad (\sin \frac{\theta}{2}) \qquad (2.4)$$

Two main conclusions may be drawn from equation (2.4): the resultant force exerted by the trochlea on the tendons (1) increases as wrist thickness decreases and (2) increases as joint angle of the wrist deviates from neutral. Therefore, tendons will be acted upon with highest resultant forces by the trochlea in small wrists that are hyper-extended or hyperflexed.

2.3 CARPAL TUNNEL SYNDROME

Carpal Tunnel Syndrome is a compression neuropathy of the median nerve as it passes through the carpal tunnel of the human wrist. It is the most common peripheral neuropathy, and it generally effects women more than men at ratios of from 2:1 to 4:1 (Brain, Wright and Wilkinson, 1947; Tanzer, 1959; Kendall, 1960; Cseuz, et al., 1966; Hymdvich and Lindholm, 1966; Phillips, 1967; Chamberlain and Corbett, 1970; Phalen, 1972; Barenko and Strelka, 1976; and Gainer, 1977). The pain usually occurs in the evening and often wakes the affected person from sleep. In advanced cases, atrophy of the thenar eminence will occur resulting in loss of motor control of the thumb.

Diagnosis

Diagnosis of CTS in advanced cases may be done quickly. Phalen (1966) states that CTS is indicated in any person with:

> "hypesthesia or paresthesia in the distribution of the median nerve in the hand or in any patient who has weakness or paralysis of the abductor pollicis brevis or opponens pollicis."

Less advanced cases may be determined through simple clinical tests. Barenco and Strelka (1975) outline four clinical tests:

1. nocturnal pain which disturbs sleep, usually associated with paresthesias, and
2. positive Tinel's test, and
3. positive Phalen's test, and
4. weakness in thumb opposition and abduction or atrophy of the thenar eminence.

Phalen (1972) has also observed that CTS is indicated by swelling on the volar side of the forearm just proximal to the wrist crease. Generally, X-rays are not a helpful method of diagnosing CTS unless prior history of bone damage is available (Phalen, 1972). Latency in nerve conduction tests has been well documented as an indicator of CTS (Barnes and Currey, 1967; Kemble, 1968; Plata, 1971).

Treatment

Relief from CTS has been accomplished using steroids injected into the wrist and by splinting the wrist in a neutral position (Phalen, 1972). In more advanced cases, particularly when thenar atrophy has occurred, surgical methods are frequently used. The methods involve sectioning the flexor retinaculum to relieve the pressure in the carpal tunnel (Barenco, 1975; Curtis, 1973; Phalen, 1972).

Etiology

Several causes have been proposed for CTS including pregnancy (Nicholas, 1971), rheumatoid arthritis (Herbison, 1973), congenital anomalies (Phalen, 1966), and ischemia of the median nerve tissues (Eversmann, 1978; Kendall, 1960). Phalen (1972) and Tanzer (1959) discovered cases where nerve compression was linked to inflammation and thickening of the synovial membranes of the finger flexor tendons. The pressure of flexor tendons against the median nerve during wrist flexion may be a contributing factor in the onset of CTS (Brain, et al., 1947; Smith, 1977).

CTS may occur due to extensive use of the hand in the industrial workplace. It has been linked to highly repetitive movements of the hand (Gainer, 1977; Hymovich, 1966; Tichauer, 1966). It has also been linked to strenuous hand use and occurs most frequently in the dominant hand (Phalen, 1972). Welch (1972) has proposed various factors in the industrial environment which predispose the worker to tenosynovitis. He includes parameters such as hand movements and forces used with tools and machinery controls. Mohr (1977) and Raybourn (1977) suggest the possibility of a relationship between CTS and job factors such as force of exertion, wrist deviation and hand position. Tichauer (1966) proposed that large stresses occur in the connective tissue of the human arm during industrial work performance. He has cited some causes of high stress as equipment control design and hand tool design. He also proposes changes which will alleviate the imposed stress.

2.4 SUMMARY AND HYPOTHESIS

CTS is a widespread problem in and out of industry. It occurs when the median nerve is compressed in the carpal tunnel of the wrist. The result of the compression is hand pain and possible atrophy of the thenar eminence resulting in complete median nerve dysfunction. Once diagnosed, the solution may be as simple as to discontinue heavy use, or it may require surgery to relieve pressure in the carpal tunnel. The exact conditions which evoke the problem have not been determined. Compression of the median nerve, however, may result from any factor which increases the pressure in the carpal tunnel and, specifically, pressure on the median nerve in the tunnel.

In industry CTS may be due to repetitive hand motions and forceful exertions. This movement predisposes the worker to tenosynovitis, the inflammation from which will cause increased pressure in the carpal tunnel with resulting chronic pressure on the median nerve. During forceful exertions with the hand in the flexed position, the finger flexor tendons directly impinge on the median nerve pressing it against the flexor retinaculum. This acute pressure on the median nerve or chronic pressure from tenosynovitis may directly result in Carpal Tunnel Syndrome in the workplace.

Forces on the tendons during wrist extension and flexion are related to the wrist size and degree of joint rotation. The hypothesis that will be tested in this paper is:

> INTRA-WRIST FORCES IMPOSED ON THE TENDON AS IT PASSES THROUGH THE CARPAL TUNNEL DURING WRIST EXTENSION AND FLEXION INCREASE SIGNIFICANTLY AS THE WRIST THICKNESS DECREASES DUE TO CHANGES IN TENDON GEOMETRY. VARIATIONS IN WRIST STRUCTURE ARE AN ETIOLOGICAL FACTOR IN THE OCCURRENCE OF CTS.

High forces on the flexor tendons in the wrist increase the probability of structural damage to soft tissues and pathology to those tendons, especially if repeated hand movements are used. Pathology such as tenosynovitis increases chronic pressure on the median nerve. When the wrist is flexed, acute forces are placed directly upon the median nerve.

This report will also attempt to show two distinct methods of determining flexor tendon geometry and compare the results of the two methods.

III. EXPERIMENTAL DESIGN

3.1 ANATOMICAL SEGMENT

The first portion of this report is concerned with the geometry of the curvature of the finger flexor tendons as they pass over the trochlea of the wrist. This geometry was estimated using two different methods. The first method used a relationship between the change in joint angle of the wrist and resulting displacement of the flexor tendon to determine the radius of curvature of the tendon as it passes over the trochlea. This radius of curvature is shown by equations 2.2 and 2.3 to be inversely related to the load and resultant force imposed on the tendon by the trochlea at a given tendon tension.

The second method involved the dissection of human cadaver limbs and direct measurement of the location of the tendon in space. Polynomials were fitted to the data and the radius of curvature of the tendon in the vicinity of the trochlea was determined.

3.1.1 TENDON-JOINT DISPLACEMENT

BACKGROUND

As described in section 2.2, the finger flexor tendons of the hand pass against the carpal bones when the hand is extended and against the flexor retinaculum when the hand is flexed. These structures then act as trochlea for the flexor tendons when the wrist is deviated from the neutral position (Figure 2-9). Landsmeer (1960) has proposed that the tendons passing against an articular surface of a joint displace as a function of the joint rotation. This relationship is described by:

$$x = r\,\theta \qquad (3.1)$$

where:

x = displacement of the tendon

r = radius of curvature of the tendon over the articular surface of the joint

θ = angle of joint rotation from the neutral position

Landsmeer also proposed two alternative models which have been shown not to apply to the interphalangeal joints (Armstrong and Chaffin, 1977).

Anatomical Materials

Four unembalmed cadaver limbs were analyzed for this report. Three hands were female, and one was male. The hands were made available from anatomical donations by the Department of Anatomy at the University of Michigan. The hands were chosen in an attempt to encompass the sizes of a diverse population of wrist sizes. The dimensions and percentile rankings of selected dimensions are listed in Table 3-1.

Equipment

A rigid metal structure was used to mount the hands. Light steel connecting line was used to link tendons to a one kilopond weight. Lead shot in a tin can served as the weight which provided tendon tension. Masking tape contorted into the shape of a marker served as an indicator of tendon displacement. Heavy carpet tape and wooden

Table 3.1 - Cadaver Hand Subject Wrist Thickness and Percentile Ranking

Subject No.	Wrist * Thickness, (mm)	Percent. Ranking	Wrist Breadth Percent. (mm)	Wrist Circum. Percent.(mm)
1	36.0	31.4	55.0	146.0
2	38.0	35.7	54.0	147.0
3 **	46.0	80.0	68.0	168.0
4	31.5	3.0	53.0	137.0

* Percentile estimated from standard wrist circumference in Garfett (1970). Circumference calculated from wrist thickness and breadth using equation:

$$c = \pi \ (a^2 + 5^2)\ /_2$$

** Male Subject

tongue depressors served to splint the fingers in a rigid position. A metric ruler and goniometer were used to measure tendon displacement and joint angle respectively.

Method

Each hand to be analyzed was mounted on a rigid structure in such a way as to allow free movement of the hand in extension and flexion (Figure 3-1). Before any experiments were done on the hands, all material up to approximately two inches proximal to the wrist crease was removed. The nine extrinsic finger flexor tendons were then isolated and a piece of light steel connecting line was attached to each tendon. The fingers of the hand were then splinted into a rigid position to insure no additional tendon displacement would

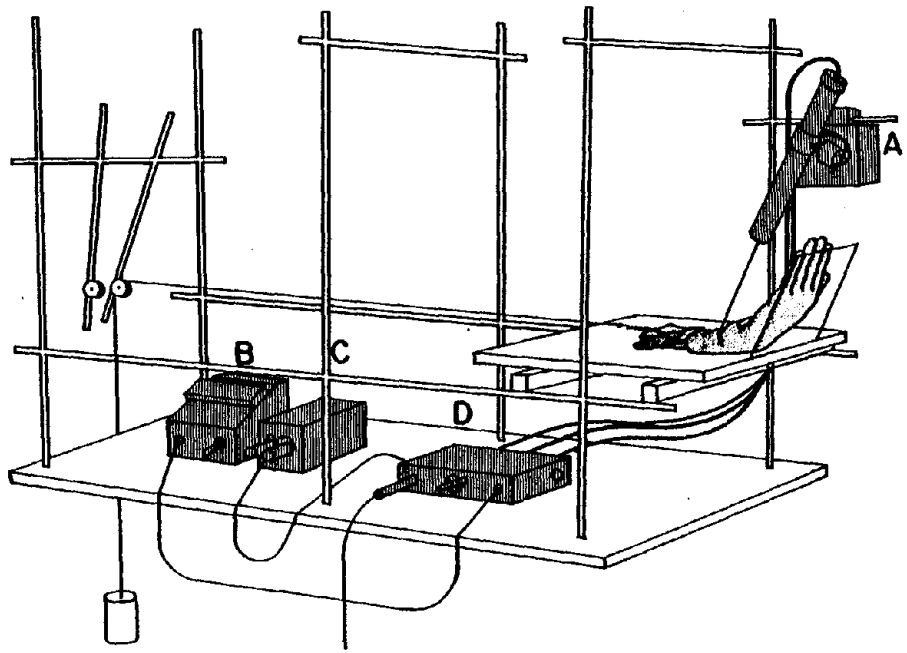

Figure 3-1: Mounting Structure for Tendon-Joint Displacement Measurements

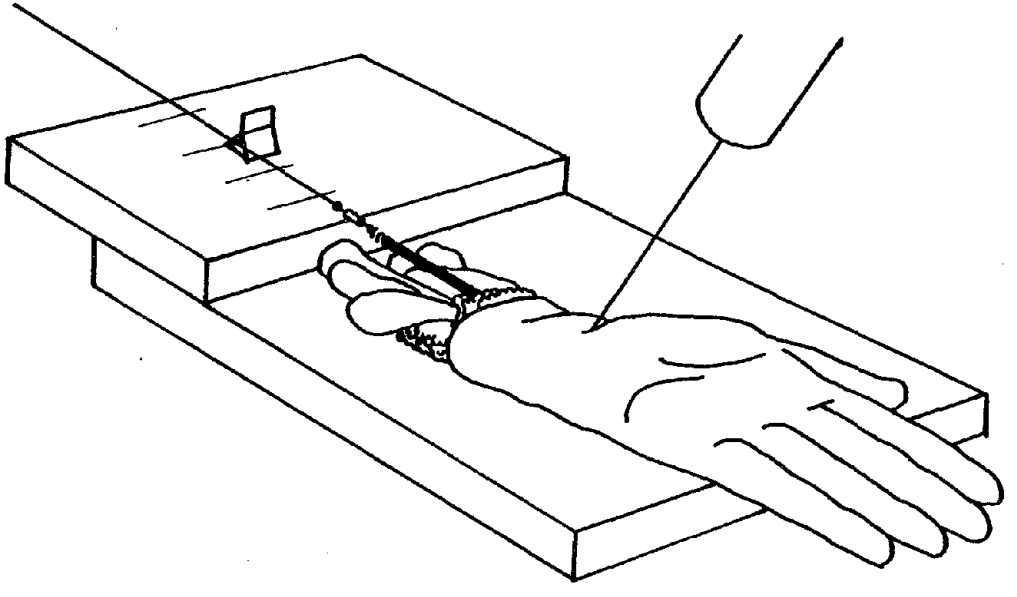

Figure 3-2: Tendon Displacement Measuring Technique

occur due to finger flexion or extension. Directly proximal to the hand a metric ruler was secured on the structure in the same plane as the palmar side of the wrist joint. A locating device was attached to the steel connecting line above the ruler to be used as an indicator of tendon displacement (Figure 3-2). A one kilopond weight was attached to the steel connecting line to provide tendon tension.

Two experimenters were used during the actual recording of data. The first experimenter used a goniometer to position the hand at the required angle of extension or flexion. The second experimenter recorded the position of the indicator on the metric ruler. Each tendon was tested separately for three to five trials. The displacement of the tendon was recorded with the hand extended fifty degreees, forty degrees, and twenty degrees, then flexed twenty degrees and forty degrees. This method gave consistent results with negligible error. Figure 3-2.5 shows the resulting recorded points in each of the three positions for hands three and four.

3.1.2 TENDON LOCATION

To gain a more direct measure of the geometry of tendon curvature through the carpal tunnel, a direct anatomical mapping of the tendon path through the carpal tunnel was attempted. The points describing this path may then be fitted with curves by the method of stepwise polynomial regression. After choosing a curve which best fits the data, the radius of curvature of the tendon through the carpal tunnel may be determined, and the forces acting on the tendons in this portion of the wrist may be described using equations 2.2 and 2.3.

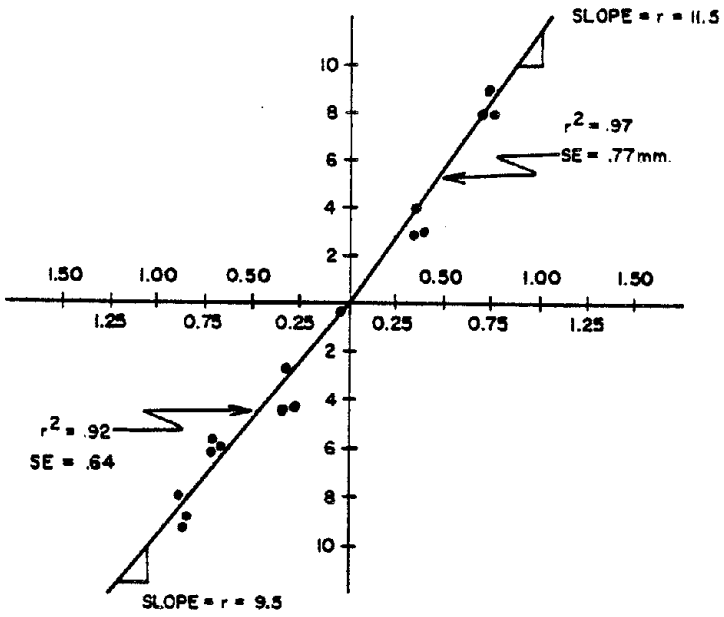

Figure 3.2.5: Plotted Tendon-Joint Displacement Points and Regression Line

Equipment

A three dimensional point encoder was used to gather tendon location data (Figure 3-3). This encoder consists of a series of three position transducers which located points in space in spherical coordinates. Two of the transducers put out a changing voltage as they are turned and were used to measure the angular components of spherical coordinates. The third transducer is a linear differential position transducer which was used to measure the radial component of spherical coordinates.

A control box in conjunction with an A.C. voltmeter were used to monitor the output voltages of the three position transducers

as they were sent to a Hewlett Packard 2100A computer to encode a point in space. It also generated an operator controlled signal to stop the encoding process.

Method

Each hand was again mounted on the rigid structure shown in Figure 3-4. Incisions were made approximately every one centimeter proximal to the wrist crease and the flexor tendons palpated. One incision was made directly between the pisiform and the hook of the hamate making a lateral section through the flexor retinaculum. Care was taken not to damage the median nerve which lies directly beneath the flexor retinaculum at this point. A final incision was made approximately one centimeter distal to the distal wrist crease. The flesh was removed from the palm of the hand in such a way that the tendons were exposed and structural alterations were avoided. The palmar aponeurosis was exposed and removed, and the flexor tendons in the hand were palpated.

The three dimensional point encoder, control box, and voltmeter were arranged as shown in Figure 3-4. Three points around the hand were first encoded to represent the X, Y and Z axis for the three-spaces in which the tendon and median nerve encoded points would be located. A reference point was then encoded which marked the location of the radial styloid process. Each tendon was then connected to a one kilopond weight. Points were encoded along the tendon beginning on the proximal end and moving distally. Each tendon path was encoded twice with the hand flexed forty-five degrees, neutral, and extended forty-five degrees (Figure 3-5).

The encoding of a point on the tendon consisted of entering the tip of the encoder into an incision, palpating the tendon to be encoded, and placing the tip of the encoder on the most palmar edge of the tendon. Then the verbal order to "encode point" was given, and an assistant experimenter pushed the button on the control box to allow the computer to accept the voltages from the encoder. These voltages were then transformed into the spherical coordinates by the computer.

Data was also collected describing the path of the median nerve through the carpal tunnel. A light weight was attached to the proximal end of the nerve to keep it taunt, but avoid damaging it or upsetting its natural path. The encoding procedure for the median nerve was identical to that for the flexor tendons. After all points were encoded, the data was stored for future analysis.

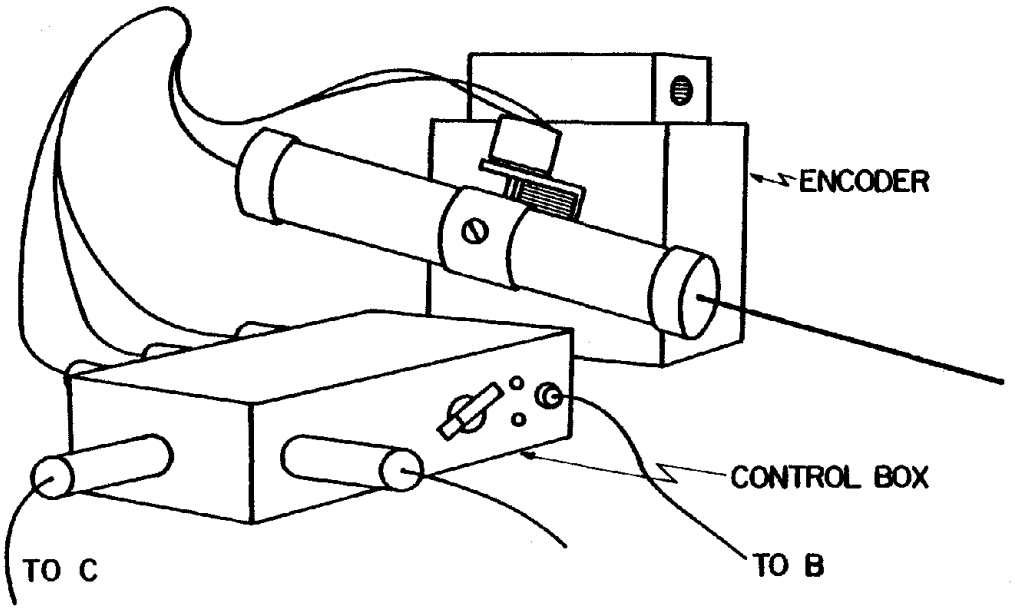

Figure 3-3: Encoding Device and Control Box

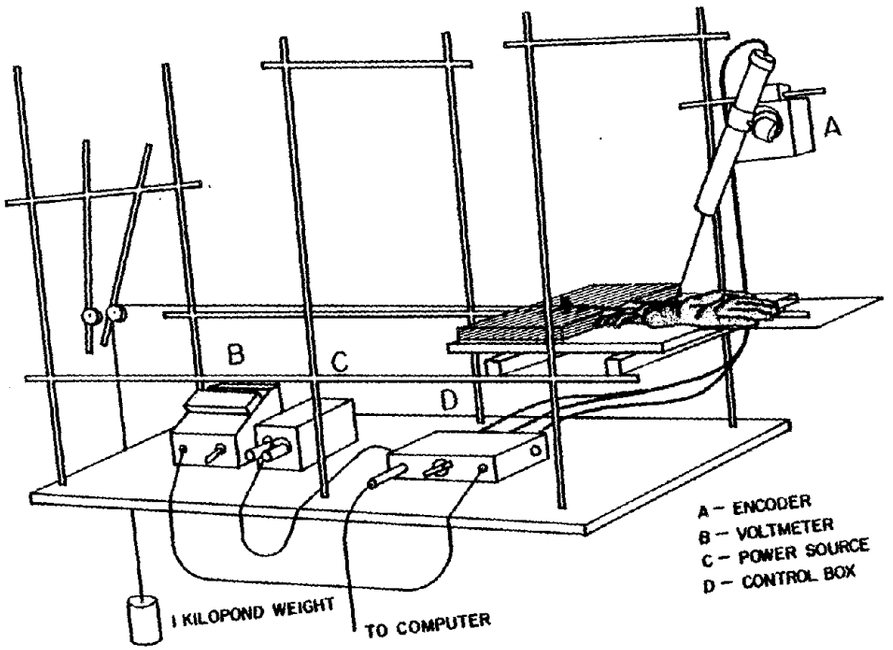

Figure 3-4: Arrangement for Collection of Tendon Location Data

3.2 RADIOGRAPHIC SEGMENT

The investigation that this report is concerned with is part of a larger project in the Human Performance Laboratory in the Industrial and Operations Department at the University of Michigan. The project has also conducted a field study in two automobile upholstery manufacturing plants to determine the etiology of carpal tunnel syndrome in industrial workers (Mohr, 1977; Rabourn, 1977). That study has generated radiographs of subjects who have a history of CTS and those who do not have a history of CTS. As part of this report, these radiographs were analyzed with two purposes in mind: to attempt to (1) discover a relationship between some bone sizes, which determine the dimensions of the carpal tunnel and the hand, and the occurrence of CTS; and (2) to determine relationships between bone lengths and link lengths for the phalanges and metacarpals of the hand for future biomechanical models.

Equipment

Mitutoyo calipers were used to take measurements off of the radiographs. The radiographs were illuminated with a flourescent light viewing table. Carpal angle was measured with a goniometer.

Method

The following five measurements were chosen in an attempt to characterize the volume of the carpal tunnel and relate bone structures of the hand and wrist to the occurrence of CTS (Figure 3-6):

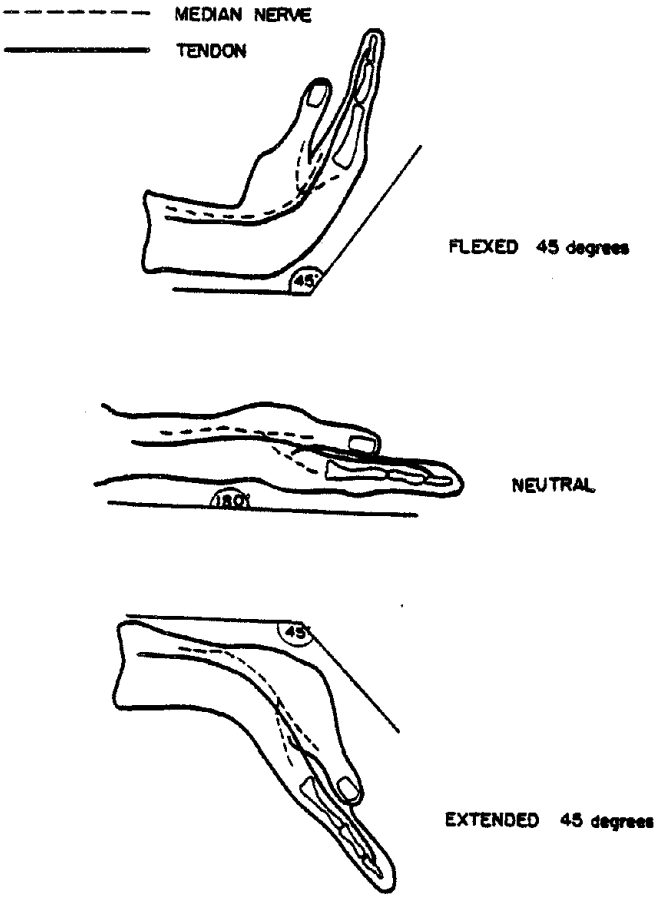

Figure 3-5: Hand Positions for Collection of Tendon Location Data (Adapted from Armstrong, 1975)

1. The distance from the medial edge of the radius to the lateral edge of the ulna at widest point. (This measurement was selected to give an indication of wrist width.)

2. The distance from the lateral edge of the tubercle of the trapezium to the medial edge of the hook of the hamate. (This measurment was selected as an indicator of carpal tunnel width.)

3. The distance from the medial edge of the trapezium to the lateral edge of the hamate. (This measurement was selected as a second indicator of carpal tunnel width.)

4. The distance from the distal edge of the radius at the anteroposterior ridge to the distal edge of the third metacarpal. (This measurement was selected as an indicator of hand length.)

5. The carpal angle. The carpal angle is the angle formed by a line drawn tangent to the lateral edges of the lunate and trequetrum, and the line drawn tangent to the medial edges of the lunate and scaphoid. (This measurement was taken as an indicator of the formation of bony structures of the wrist, Harper, et al., 1974).

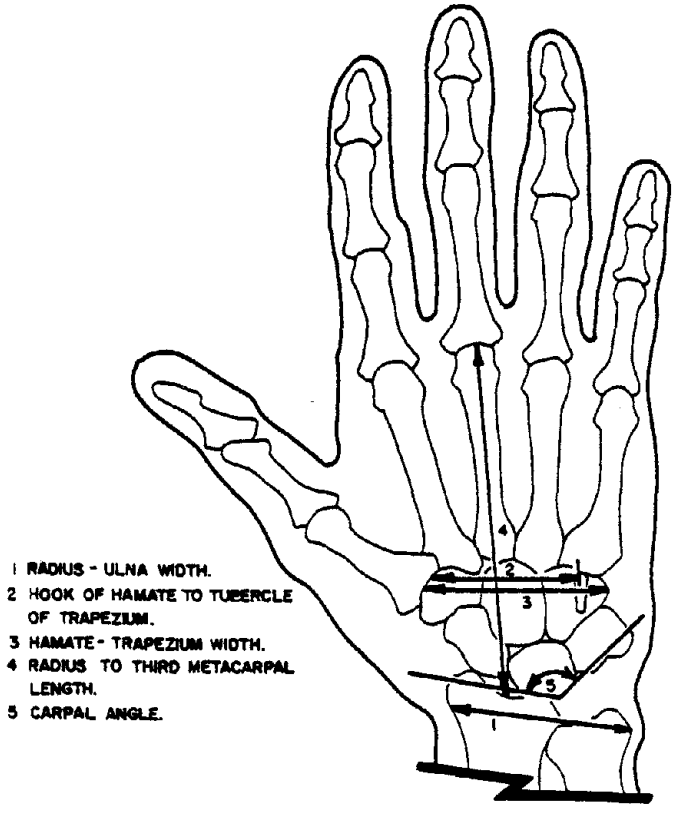

Figure 3-6: Wrist and Hand Measurements

These five measurements were taken off of each radiograph for each subject. All of the radiographs were 1:1 scale.

The bone lengths of each of the phalanges and metacarpals were measured for each subject (Figure 3-7). The lengths were measured from the distal end of the bone to the proximal end as described by Poznanski (1974). The corresponding link lengths were also measured. The joint centers were estimated by observing a skeletal structure of the hand, determining where the joint centers were for each bone and relating this location to the radiographs (Figure 3-8).

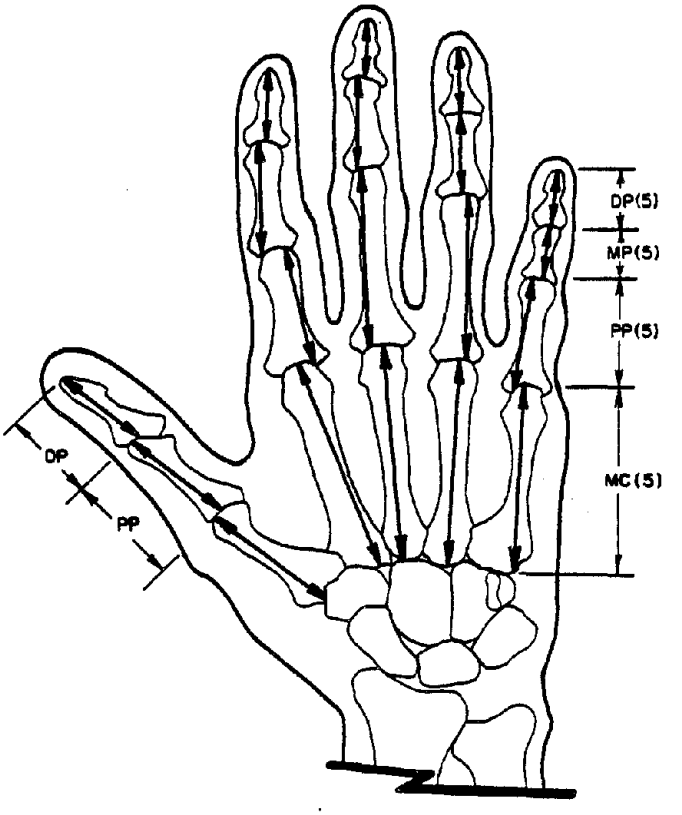

Figure 3-7: Phalange and Metacarpal Bone Length Measurements

The joint center for the wrist was taken as the lateral point of the lunate-capitate articulation. These measurements were to be used to develop a predictive model of link length from bone length for the phalanges and metacarpals of the hand.

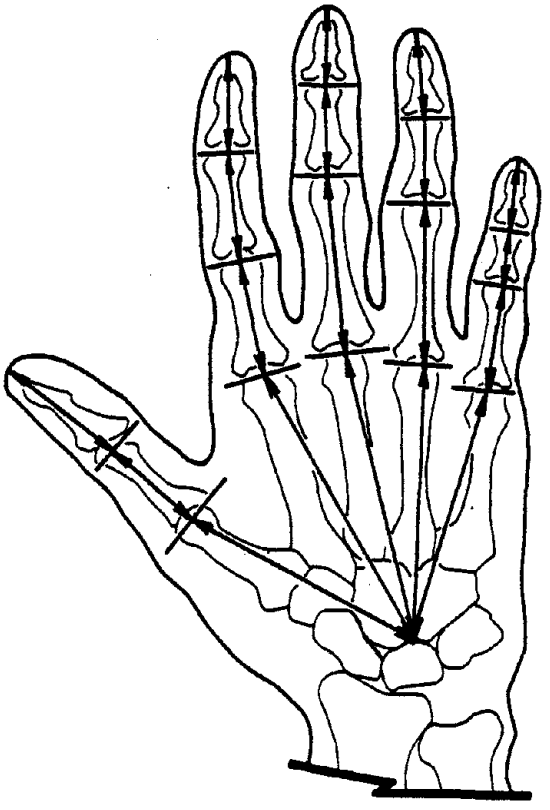

Figure 3-8: Corresponding Phalange and Metacarpal Link Length Measurements

IV. RESULTS

4.1 ANALYSIS OF DATA

Data were collected for this report using three different methods, and the analysis of the data are designed to best accomplish the specific objective of each method. The data from tendon-joint displacement measurements and tendon location measurements were analyzed in an attempt to characterize the radius of curvature of the tendon as it passes through the carpal tunnel. Measurements from radiographs of hands and wrists of subjects with CTS and those without the syndrome were analyzed (1) in an attempt to correlate the bone structure of the wrist with the occurrence of CTS, and (2) in an attempt to develop a predictive model of link length from bone length as seen in the radiographs. All statistical analysis was done with the aid of the Michigan Interactive Data Analysis System (MIDAS).

4.1.1 TENDON-JOINT DISPLACEMENT

Tendon displacement was recorded as a function of wrist joint rotation for each hand. This was done in an attempt to determine the radius of curvature for each tendon from equation 3.1. The data were separated into two groups corresponding to when the hand was flexed and extended. Armstrong and Chaffin (1977) have shown that the radius of curvature for the flexor tendons differs between extension and flexion. Least squares linear regression through the origin was used to find a relationship between tendon displacement and joint rotation. The resulting radius of curvature (r) values for each tendon of each hand are shown in Table 4-1 through Table 4-4.

Table 4-1 Sagittal Plane r mm Valve Observed from Tendon-Joint Displacement Measurements for Hand 1.

	Extended Wrist		Flexed Wrist	
Digit	FDS	FDP	FDS	FDP
1	NA*	11.46mm	NA	13.56mm
2	10.47mm	12.78mm	13.89mm	12.41mm
3	9.51mm	7.64mm	11.46mm	13.75mm
4	10.65	6.37mm	13.37mm	15.47mm
5	*	6.78mm	*	15.09mm

*The FDS 5 tendon was not analyzed because of its small size and lack of contribution to carpal tunnel pressures.

Table 4-2 - Sagittal Plane (mm) values from tendon-joint displacement measurements for Hand 2.

	Extended Wrist		Flexed Wrist	
Digit	FDS	FDP	FDS	FDP
1	NA	10.85	NA	15.28
2	11.05	9.89	17.00	17.57
3	11.32	8.80	18.72	16.23
4	8.73	7.43	16.43	15.85
5	*	6.96	*	14.52

Table 4-3: Sagittal Plane r (mm) values from Tendon-Joint Displacement Measurements for Hand 3

	Extended Wrist		Flexed Wrist	
Digit	FDS	FDP	FDS	FDP
1	NA	10.74	NA	22.92
2	11.94	10.37	21.00	18.53
3	11.53	10.50	17.38	17.38
4	9.69	9.21	19.67	19.67
5	*	8.66	*	18.91

* The FDS 5 tendon was not analyzed because of its small size and lack of contribution to carpal tunnel pressures.

Table 4-4: Sagittal Plane r (mm) values from Tendon-Joint Displacement Measurements for Hand 4

	Extended Wrist		Flexed Wrist	
Digit	FDS	FDP	FDS	FDP
1	NA	11.75	NA	9.63
2	9.64	9.40	11.19	10.84
3	10.03	9.84	10.21	10.01
4	8.98	9.36	9.02	8.72
5	9.17	7.83	9.54	9.97

Armstrong and Chaffin (1977) also showed common trends in r values for FDS and FDP tendons in both flexion and extension. He proposes a predictive model to determine tendon displacement as a function of wrist angle and wrist thickness:

$$\text{Average Radius of Curvature} \quad (MM) = 1.507 + 2.89\,W_2 + 6.07W_3 - .55\,W_2W_4 \qquad (4.1)$$

W_2 = wrist thickness (CM)

W_3 = 0 - extension/1 - flexion

W_4 = 0 - superficialis/1 - profundus

Table 4.5 shows average r values for FDS and FDP in extended and flexed positions in comparison with predicted r values from equation 4.1.

Table 4.5: Sagittal Plane Radius of Curvature (mm) Observed from Tendon-Joint Displacement. Measured and Calculated from Eq. 4.1*

		Extended		Flexed	
		Superficialis	Profundus	Superficialis	Profundus
Hand 1	Observed	10.2 mm	9.0 mm	12.9 mm	14.1 mm
	Predicted	11.8 mm	9.9 mm	17.9 mm	16.0 mm
Hand 2	Observed	10.4	8.8	17.4	15.9
	Predicted	12.4	10.3	18.5	16.4
Hand 3	Observed	11.0	9.9	19.4	19.5
	Predicted	14.7	12.2	20.8	18.2
Hand 4	Observed	9.5	9.6	10.0	9.8
	Predicted	10.6	8.9	16.7	14.9

* Radius of curvatures in mm

4.1.2 TENDON LOCATION

Points were encoded along the path of each flexor tendon as the hand was flexed forty-five degrees, neutral, and extended forty-five degrees. Figure 4-1 shows a plot of points along the FDP tendon for digit five and the FPL tendon for hand number 1. These points are superimposed upon an outline of hand number 1 taken from a radiograph of that hand. These points describe the medial and lateral boundries of the carpal tunnel as seen from the palmar view.

The flexor tendons were analyzed and the minimum radius of curvature was determined in two planes corresponding to a coronal (palmar) and sagittal (lateral) view of the wrist (Figure 4-2). The radius of curvature which is reported for each tendon was calculated from the individual curve which was fitted to each tendon. The equation for the radius is:

$$R = \frac{1+(y(x)')^2)^{1.5}}{y(x)''}$$

Where: $y(x)'$ = first derivative of fitted curve

$y(x)''$ = second derivative of fitted curve

Figure 4-3 shows a simulated path of the tendon as it passes through the carpal tunnel. The tendon curves in the coronal plane (XY) as well as the sagittal plane (XZ). The radius of curvature for each tendon is calculated along the path of the tendon in the

Figure 4-1: FDL and FDP5, Tendon Paths Bounding the Carpal Tunnel

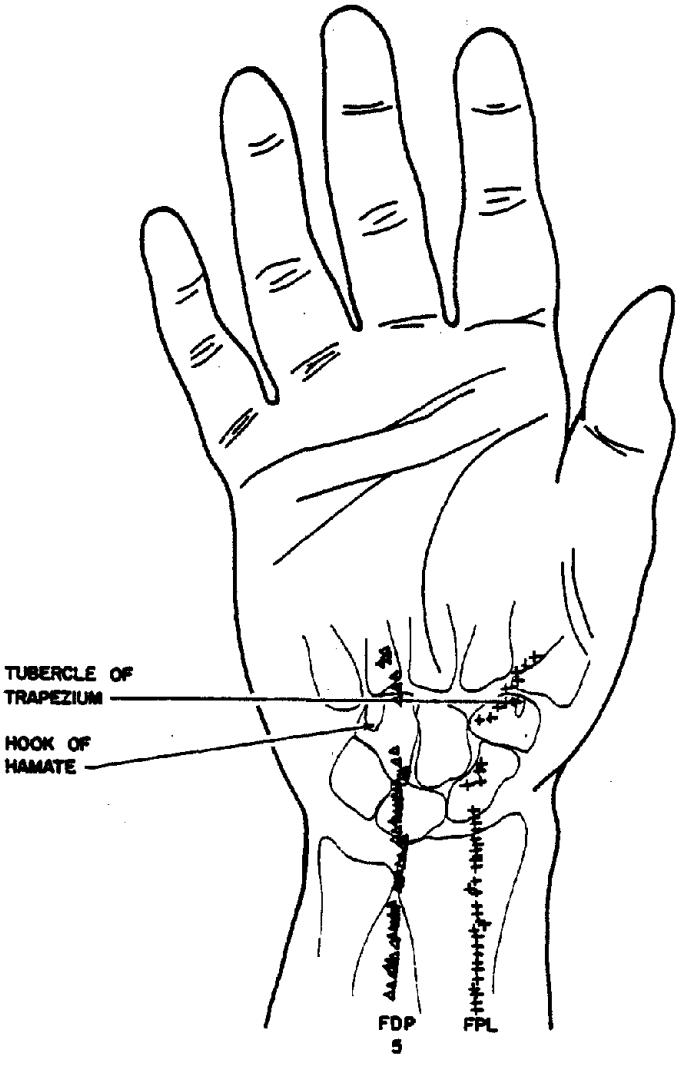

sagittal plane for the wrist flexed, neutral, and extended and it is calculated in the coronal plane for the wrist neutral.

Table 4-6 shows the minimum radius of curvature (r_{min}) as given by third, fourth, and fifth order polynomials when fitted to the encoded data points of hand 2. The polynomials were fitted to the points in the vicinity of the radial styloid process to facilitate a good fit of the curves at the trochlea, which is the location of interest. Least squares polynomial regression was used to fit the curves to the data. The error of regression along with the minimum

Figure 4-2: Coronal (XY) and Sagittal (XZ) Planes

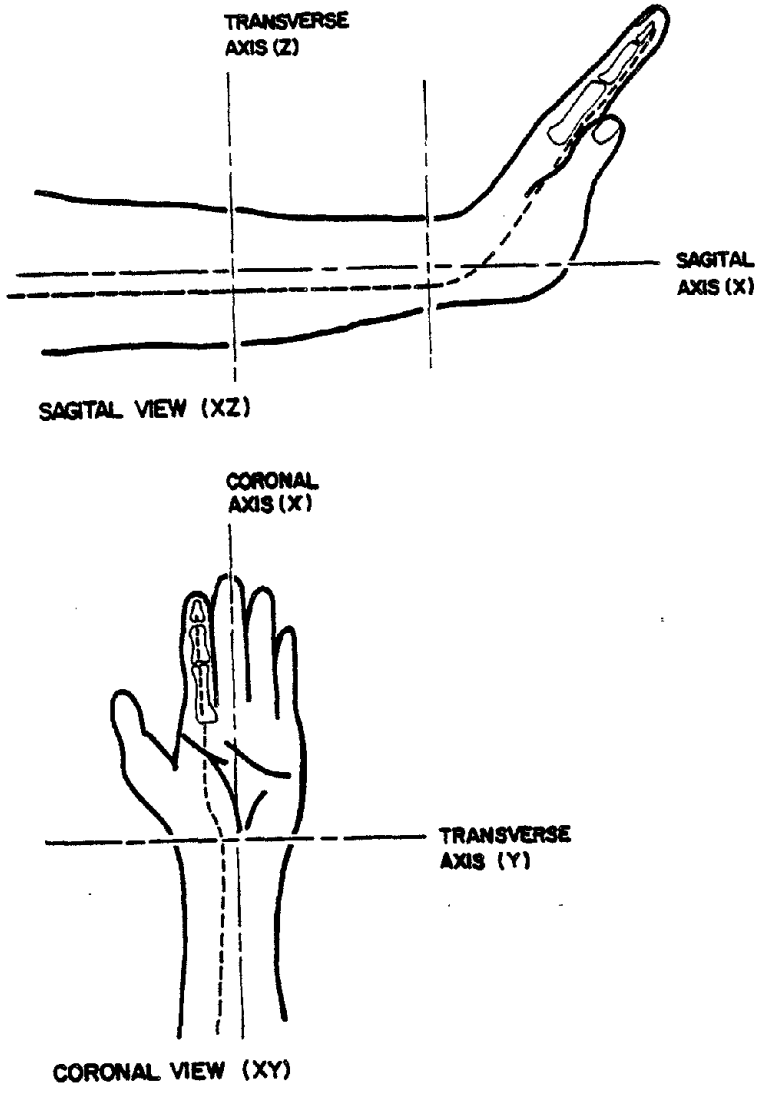

radius of curvature and the location of that minimum along the tendon is recorded for the hand in the flexed, neutral, and extended position. Where no minimum radius of curvature was indicated by the fitted curves in the area of interest on the tendon, an asterisk (*) is placed above the recorded r_{min}. The r value in these cases was taken as representative of r values in the vicinity of the trochlea. Table 4-6 also shows the minimum radius of curvature, location of that minimum, and the error of regression when piecewise polynomials were

Figure 4-3: Tendon Radius of Curvatures in XY and XZ Planes

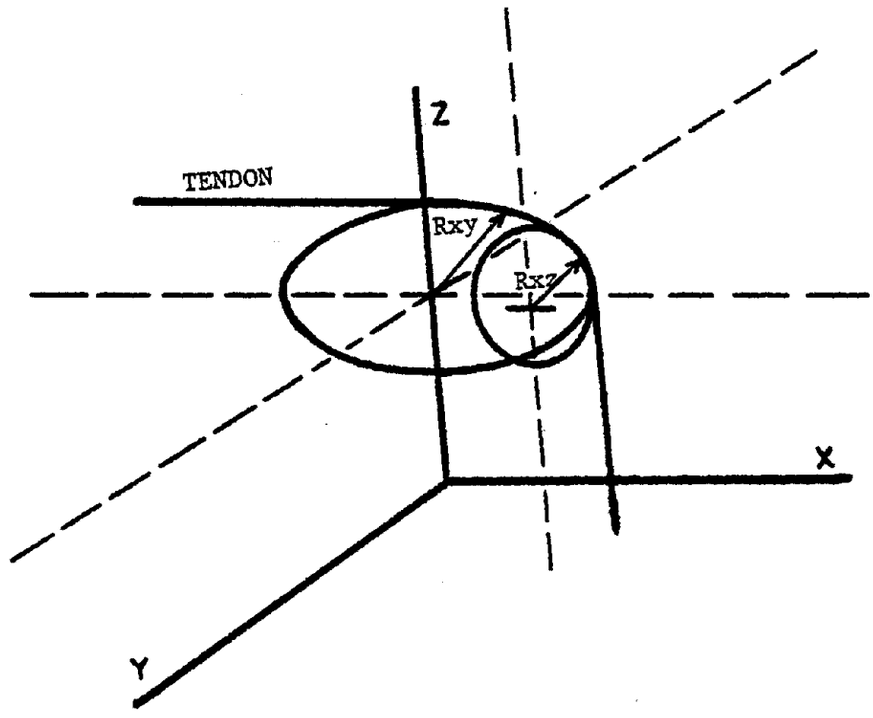

Table 4-6 - Sagittal Plane Flexor Tendon-Geometry of Hand 2 - Data in Cm.

Wrist Position	Tendon		POLYNOMIAL 3rd Order R-xz	Xrmw	Error	POLYNOMIAL 4th Order Rx-z	Xrmw	Error	SPLINES 5th Order Rx-z	Xrmw	Error	Rx-z	Xrmw	Error	T-I RMIN (CM)
Flexion	FDS	2	4.28	10.0	.056	5.85	12.4	.050	4.24	12.2	.048	6.46	13.6	.046	1.70
		3	4.30	11.0	.052	5.36	12.2	.044	3.97	12.1	.039	2.78	[illegible]	.036	1.87
		4	4.57	10.0	.055	5.45	12.3	.053	3.91	12.1	.049	2.75	[illegible]	.045	1.64
		5													
	FDP	1	7.00	11.0	.050	6.11	12.5	.048	6.23	12.6	.050	6.34	14.5	.039	1.53
		2	5.39	11.0	.068	5.4*	11.0	.069	3.95	12.0	.066	3.02	12.2	.064	1.76
		3	6.10	14.10	.085	5.08	13.3	.085	3.94	13.5	.085	2.33	[illegible]	.068	1.62
		4	7.80	13.50	.083	5.33	12.9	.081	4.86	13.3	.081	2.76	[illegible]	.082	1.59
		5	6.32	13.7	.048	4.58	12.6	.042	3.88	12.0	.040	3.02	[illegible]	.030	1.45
Neutral	FDS														
		2	33.0*	14.6	.060	23.30	15.7	.061	8.87	14.5	.055	13.9	16.1	.047	
		3	32.77*	14.6	.034	36.6*	14.6	.035	15.5	12.9	.036	10.3	14.1	.037	
		4	18.9*	14.6	.112	8.18	15.1	.107	8.06	15.0	.111	6.34	16.8	.102	
	FDP	1	75.0*	15.0	.055	105.2*	15.0	.56	28.01	14.4	.056	29.63	14.0	.05	
		2	15.86*	14.6	.052	13.03	14.2	.052	16.98*	14.6	.054	4.07	16.0	.075	
		3	52.2*	15.0	.072	29.8	14.9	.071	10.72	14.3	.070	8.56	13.9	.067	
		4	22.6*	14.6	.051	13.24	15.3	.051	12.14	16.0	.053	8.24	16.2	.051	
		5	41.0*	14.6	.070	12.84	15.1	.070	13.28	13.7	.068	9.17	17.3	.059	
Extension	FDS	2	3.72	13.2	.076	3.40	13.9	.076	3.78	14.5	.077	2.70	15.0	.055	1.11
		3	1.72	12.8	.123	2.45	14.0	.103	2.79	14.0	.106	1.98	14.3	.068	1.32
		4	1.68	12.5	.082	2.80	13.4	.069	2.41	13.5	.072	1.82	14.4	.051	.87
		5													
	FDP	1	1.89	13.0	.152	1.35	12.0	.117	0.82	12.4	.108	2.76	15.1	.095	1.09
		2	3.79	14.1	.064	2.94	14.2	.061	3.02	15.0	.059	2.85	13.9	.050	.99
		3	2.30	12.6	.133	2.41	13.7	.127	3.01	14.7	.116	2.81	14.5	.079	.88
		4	2.46	12.5	.101	2.59	14.0	.076	2.57	13.9	.079	1.66	14.3	.065	.74
		5	3.34	12.0	.069	3.90	13.2	.065	5.04	14.8	.068	2.69	14.5	.049	.70

fitted to the data. This method is called the method of splines and is described by Lee (1978). Splines facilitates the analysis of the data by allowing the placement of knots at desired intervals along the path of the data points. Between each pair of knots, a third order polynomial was fitted to the data. Points which occur on the knots are included in the polynomials on either side of the knot. Finally, Table 4-6 gives the radius of curvature indicated by the tendon-joint desplacement analysis for hand 2 to facilitate comparison of the three methods used to descrive the radius of curvature of the flexor tendons in the vicinity of the trochlea.

Tables 4 through 9 show the minimum radius of curvature, location of that minimum and the error of regression for polynomial regression, and the method of splines applied to hands 1, 3, and 4 respectively. The data are in the sagittal plane, and the polynomials are third order. Again, where no r_{min} was found, an asterisk (*) indicates a representative r_{min} value.

Table 4-10 gives the minimum radius of curvature, the location of that minimum, and the error of regression for the data points in the coronal (XZ) plane. All four hands are given in the neutral position, and again, third order polynomials and the method of splines are used.

The corresponding sagittal plane location data for the median nerve of each hand are given in Table 4-11. Its geometry is described with the hand in the flexed, neutral, and extended positions for all four hands. Figure 4-4 shows a coronal plane plot of the FDP tendons for digits 2 through 4 and the median nerve with the hand in a neutral position.

Table 4-7 - Sagittal Plane Flexor Tendon Geometry, Hand 1 - Data in Cm.

			Polynomial 3rd Order			Splines		
			RMW	XRMW	Error	RMIN	XRMW	Error
Flexion	FDS	2	10.48	17.5	.048	7.43	16.3	.041
		3	11.61	13.0	.023	8.94	16.8	.025
	FDP	1	6.92	16.4	.031	5.37	16.1	.022
		2	4.62	12.8	.033	4.83	15.1	.022
		3	3.69	12.2	.038	4.86	13.7	.030
Neutral	FDS	2	20.78	14.3	.034	7.7	17.4	.023
		3	20.88*	16.0	.025	18.93	18.3	.023
	FDP	1	98.2*	16.0	.022	45.1	13.9	.016
		2	47.76*	16.0	.030	20.1	16.9	.025
		3	23.95*	16.0	.072	96.9	16.0	.069
Extension	FDS	2	3.05	16.0	.028	2.19	16.5	.044
		3	3.79	16.3	.039	2.88	17.2	.037
	FDP	1	5.71	17.0	.046	3.70	16.8	.032
		2	2.14	15.0	.038	2.04	15.9	.053
		3	3.18	14.1	.037	3.62	16.2	.071

Table 4-8 - Data from Sagittal Plane Flexor Tendons, Hand 3, in Cm.

			POLYNOMIAL 3rd ORDER			SPLINES		
			RMW	XRMW	Error	RMW	XRMW	Error
Flexion	FDS	2	3.76	13.6	.108	4.09	12.5	.063
		3	1.45	11.5	.081	2.07	12.7	.050
		4	3.03	11.0	.103	4.06	11.1	.084
	FDP	1	3.58	13.2	.068	2.73	12.1	.045
		2	3.02	10.7	.066	2.92	12.62	.048
		3	6.38	13.9	.078	2.45	12.7	.059
		4	2.84	10.2	.068	5.34	12.5	.051
		5	5.97	10.0	.087	5.65	12.2	.064
Neutral	FDS	2	21.21*	14.0	.063	10.5	15.9	.043
		3	25.08	14.0	.034	25.9	12.0	.083
		4	48.03	14.0	.025	16.5	12.9	.041
	FDP	1	36.49	14.0	.053	2.84	16.1	.073
		2	38.88	14.0	.044	10.6	12.3	.047
		3	22.16	14.0	.048	8.6	12.1	.083
		4	22.45	14.0	.049	16.6	12.1	.050
		5	23.71	14.0	.041	4.97	17.8	.070
Extension	FDS	2	3.21	11.7	.063	3.14	12.7	.061
		3	3.79	10.5	.081	2.57	12.6	.070
		4	2.58	11.8	.061	2.84	12.5	.085
	FDP	1	2.47	12.0	.038	3.14	12.5	.048
		2	2.20	12.2	.060	4.01	13.1	.082
		3	2.29	12.1	.078	2.74	12.2	.055
		4	3.71	11.5	.057	3.37	12.5	.040
		5	3.1	11.4	.041	2.19	11.52	.045

Table 4-9: Sagittal Plane Flexor Tendon - Geometry, Hand 4, in Cm.

			SPLINES			POLYNOMIALS 3rd ORDER		
			RMW	XRMW	Error	RMW	XRMW	Error
Flexion	FDS	2	2.13	19.81	.090	2.45	18.5	.063
		3	4.15	12.02	.058	5.08	12.8	.098
	FDP	2	4.46	14.55	.128	1.75	11.6	.042
		3	3.73	12.89	.063	2.17	11.0	.081
Neutral	FDS	2	64.66	23.1	.044	13.5*	13.0	.094
		3	140.9*	12.2	.027	45.6	11.0	.032
	FDP	2	19.89	12.0	.103	35.9*	13.0	.019
		3	236.9*	15.15	.046	154.5*	13.0	.050
Extension	FDS	2	2.93	14.04	.086	3.69	12.6	.210
		3	2.95	12.57	.052	5.38	12.7	.060
	FDP	2	3.68	12.57	.044	4.37	12.6	.099
		3	3.02	12.36	.088	1.89	10.90	.171

Table 4-10 - Coronal Plane Tendon - Geometry, Hands 1-4 in Cm.

			POLYNOMIAL 3rd ORDER			SPLINES		
Hand	Tendon	Finger	RMW	XRMW	Error	RMW	XRMW	Error
1	FDS	2	88.62*	15.0	.066	65.58	17.0	.041
		3	11.3*	15.0	.072	59.64	17.0	.067
	FDP	1	6.50	18.0	.051	1.99	18.46	.033
		2	13.12*	15.0	.057	9.07	15.89	.057
		3	11.09*	15.0	.116	64.2	17.0	.119
2	FDS	2	53.14*	15.0	.078	12.88	13.67	.051
		3	28.53*	15.0	.068	95.23	14.11	.067
		4	12.9*	15.0	.085	5.44	16.8	.051
	FDP	1	7.71	15.3	.108	2.22	15.63	.073
		2	44.52*	15.0	.095	8.27	12.17	.087
		3	14.11*	15.0	.090	11.19	16.80	.095
		4	6.78	12.8	.088	3.28	16.16	.098
		5	6.67	13.8	.107	3.36	16.37	.094
3	FDS	2	48.85*	15.0	.086	--	--	--
		3	40.49	15.0	.088	25.89	12.03	.083
		4	20.1*	15.0	.060	16.51	12.86	.041
	FDP	1	6.10	15.9	.109	2.84	16.09	.073
		2	36.32*	15.0	.070	10.6	12.3	.047
		3	104.6*	15.0	.098	8.57	12.12	.083
		4	20.6*	15.0	.079	16.57	12.09	.050
		5	7.52	16.0	.099	4.97	16.75	.070
4	FDS	2	15.3*	20.0	.119	22.16*	21.9	.86
		3	37.0*	12.0	.064	36.9	12.2	.078
	FDP	2	11.6	13.8	.025	18.03*	15.4	.077
		3	23.3*	12.0	.088	22.33	11.8	.112

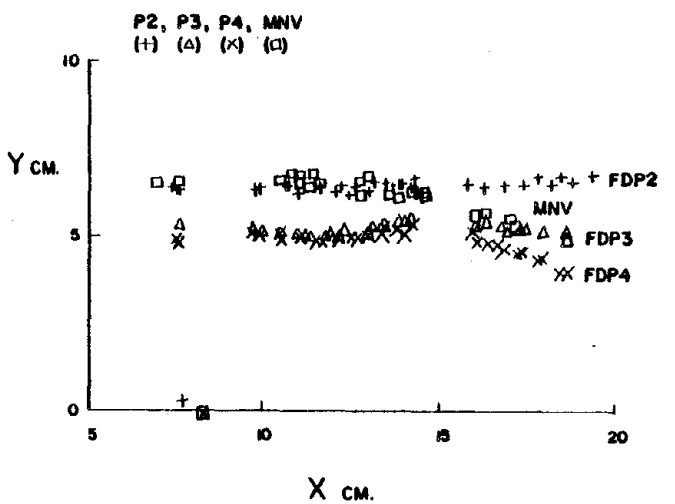

Figure 4-4; Coronal Plane View of Encoded Points for FDP2, FDP3, FDP4, and the Median Nerve from Hand Two

Table 4-11: Sagittal Plane Median Nerve - Geometry, Hands 1-4

	Flexion			Neutral			Extension		
Hand	RMW	XRMW	Error	RMW	XRMW	Error	RMW	XRMW	Error
1	6.73	17.83	.041	8.72	16.44	.043	2.34	15.31	.047
2	3.18	12.00	.109	5.78	14.13	.059	3.08	16.54	.049
3	2.45	14.30	.088	6.91	12.25	.051	1.92	12.35	.088
4	5.61	8.15	.211	8.85	8.68	.164	8.79	8.57	.048

4.1.3 RADIOGRAPH MEASUREMENTS

Wrist Measurements

Radiographs of ninety-six CTS, control and other normal subjects, were analyzed from populations described in section 3.2 of this report. Five measurements were taken which define bone dimensions of the wrist (see section 3.2.1). Since the bone structures form much of the boundary of the carpal tunnel, bone structures may reveal an etiological factor in the occurrence of CTS. A summary of the mean dimensions and standard deviation error are given in Table 4-12. The dimensions for pooled populations of CTS and control subjects are listed in Table 4-13. The level of significance (α) from a paired t-test for testing the null hypothesis that the dimensions of the two populations are the same is listed next to the control and CTS means for plant and pooled populations.

Bone and Link Lengths

From the radiographs of the populations described above, the bone

Table 4-12 - Wrist and Hand Dimension Statistics for Plants I & II

PLANT		I TECUMSEH					II. LIVONIA				
Measurement (mm)		CTS	Control	α_I	Normal	Pooled Normal	CTS	Control	α_{II}	Normal	Pooled Normal
1.	Radius-Ulna Width	47.03 ± 2.39	46.66 ± 2.84	.72	48.00 ± 2.60	47.27 ± 2.77	45.87 ± 3.08	46.67 ± 1.55	.48	46.95 ± 2.73	46.78 ± 2.35
2.	Hook Hamate Tub. Trapezium	32.52 ± 1.3	31.97 ± 1.60	.33	33.20 ± 1.69	32.53 ± 1.74	31.54 ± 1.80	31.32 ± 1.54	.79	31.14 ± 1.89	31.16 ± 1.73
3.	Ham - Trap. Width Radius - Met.	47.49 ± 1.93	46.68 ± 2.63	.45	47.67 ± 3.46	47.13 ± 3.03	48.82 ± 2.54	49.66 ± 4.20	.65	49.53 ± 2.94	49.51 ± 3.31
4.	Carpal #3 leng. Carpal	94.95 ± 3.79	93.75 ± 5.61	.51	97.33 ± 4.33	95.39 ± 5.31	95.10 ± 4.24	95.82 ± 3.02	.70	96.56 ± 4.36	96.26 ± 3.84
5.	Angle (neg)	128.2 ± 9.3	124.4 ± 9.8	.18	129.7 ± 11.2	126.8 ± 10.6	133.0 ± 8.56	127.5 ± 8.6	.15	134.2 ± 8.4	131.3 ± 9.3

Table 4-13 - Wrist and Hand Dimension Statistics for Plants I & II, Pooled

Plants I & II Pooled				
Measurement (mm)		CTS	Pooled Controls	Signif α I & II
1.	Radius-Ulna Width	46.32 ± 2.96	46.67 ± 2.40	.96
2.	Hook Hamate Tub. Trapezium	32.06 ± 1.67	31.76 ± 1.56	.35
3.	Ham - Trap Width	47.74 ± 2.37	47.79 ± 3.45	.91
4.	Radius - Meta-carpal #3 leng.	94.81 ± 3.90	94.52 ± 4.84	.68
5.	Carpal Angle (neg.)	129.8 ± 9.0	125.8 ± 9.4	.05

lengths and corresponding link lengths for the five metacarpals, five proximal phalanges, four middle phalanges, and five distal phalanges of the hand were measured and recorded. This collection was done in an attempt to construct a predictive model of link length from the corresponding measured bone length.

Five models were used to develop a predictive model for link length from bone length:

Model I: Simple linear regression model (SLRM).

Model II: Stepwise selective linear regression testing the significance of the constant (intercept) difference in link length among the five digits.

Model III: Stepwise selective linear regression testing the significance of the rate of change (slope) difference in link length among the five digits.

Model IV: Stepwise selective linear regression testing the significance of constant and rate of change differences in link length among the five digits fitting the resulting regression line through the origin.

Model IV: Stepwise selective linear regression testing the significance of constant and rate of change differences in link length among the five digits.

The general multivariate equation from which models II through V were derived is:

$$\text{Link Length (mm)} = b_o + b_1 BL + \sum_{i=1}^{5} b_{i+1} (Di - D3) + \sum_{i=1}^{5} b_{i+6} (D_i - D_3) BL \pm \text{error}$$

b_i (i=6-9) = Difference in slope between digit x SLRM and digit 3 SLRM

$B^L x$ = Bone length variable (in .1mm)

Dj-D3 = Partial regression coefficient main effects

BL(Dj-D3) = Partial regression coefficient interactions (j = 1-5)

The five models above were applied to the distal, middle and proximal phalanges and to the metacarpals. The resulting coefficients are listed in Tables 4-14 through 4-17, respectively. Significant coefficients are listed, and insignificant coefficients are listed as zero. Coefficients not applicable to a given model are shaded. The standard error of regression in .1mm is also listed under the coefficients for each model.

Table 4-14 - Link Length Predictor Models for Distal Phalange

Variable	Model I	Model II	Model III	Model IV	Model V
Constant	2.12	74.08	73.84		70.61
BL	1.37	.973	.975	1.39	0.99
D1 - D3	**	14.92		0.00	14.01
D2 - D3	**	-6.33		0.00	-6.21
D4 - D3	**	-4.92		87.93	0.00
D5 - D3	**	-19.07		60.00	0.00
BL (D1 - D3)	**		.070	0.00	0.00
BL (D2-D3)	**		-.039	0.00	0.00
BL (D4 - D3)	**		-.029	-.528	-0.03
BL (D5 - D3)	**		-.122	-.454	-0.12
Standard Error	10.34	7.58	7.62	8.77	7.58
r^2.	.92	.96	.96	.94	.96

** These variables not considered in this model.

Table 4-15 Link: Length Predictor Models for the Middle Phalange

	Model I	Model II	Model III	Model IV	Model V
Constant	2.96	0.94	1.15		0.94
BL	1.04	1.04	1.04	1.05	1.04
D1 - D3		-----		---	---
D2 - D3		4.20		4.27	4.20
D4 - D3		0.00		0.00	0.00
D5 - D3		0.00		0.00	0.00
BL (D1 - D3			0.00	0.00	0.00
BL (D2 - D3)			0.02	0.00	0.00
BL (D4 - D3)			0.00	0.00	0.00
BL (D5 - D3)			0.00	0.00	0.00
Standard Error (11mm(	6.61	6.37	6.38	6.36	6.37
r^2	.98	.98	.98	.98	.98

Table 4-16 - Link Length Predictor Models for the Proximal Phalange

Variable	Model I	Model II	Model III	Model IV	Model V
Constant	-1.41	14.58	14.13		14.13
BL	1.07	1.03	1.03	1.07	1.03
D1 - D3		-10.12		42.62	0.00
D2 - D3		0.00		0.00	0.00
D4 - D3		-4.13		0.00	0.00
D5 - D3		0.00		0.00	0.00
BL (D1-D3)			-0.03	-0.16	-0.03
BL (D2 - D3			0.00	0.00	0.00
BL (D4 - D3)			-0.01	-0.01	-0.01
BL (D5 - D3)			0.00	0.00	0.00
Standard Error (.1mm)	10.39	9.79	9.75	9.80	9.75
r^2	.97	.98	.98	.98	.98

Table 4 - 17 - Link Length Predictor Models for the Metacarpal

Variable	Model I	Model II	Model III	Model IV	Model V
Constant	361.47	138.5	144.79		138.51
BL	0.66	1.01	1.00	1.23	1.01
D1 - D3		111.24		227.31	111.24
D2 - D3		0.00		134.80	0.00
D4 - D3		0.00		109.81	0.00
D5 - D3		0.00		106.93	0.00
BL (D1-D3)			0.25	-0.17	0.00
BL (D2 - D3)			0.00	-0.21	0.00
BL (D4 0 D3)			0.00	-0.16	0.00
BL (D5 - D3)			0.00	-0.15	0.00
Standard Error (.1mm)	36.15	17.15	17.28	17.37	17.15
r^2	.72	.94	.94	.94	.94

V. Discussion

5.1 EFFECTS OF TENDON GEOMETRY

The geometry of the flexor tendons as they pass over the carpal bones or the flexor retinaculum will determine the force loadings on the tendon when it is wrapped over the trochlea. The relationship between radius of tendon curvature and load on the tendon is an inverse one as described by equation 2.2. Table 5-1 presents a summary of the mean radius of curvature of the flexor tendons in the flexed and extended positions. Tendon-joint displacement estimates of the radius of curvature are average values over the angle of extension or flexion. The tendon location estimates of the radius of curvature are values from data with the hand positioned at forty-five degrees extended or flexed. The two methods, then, are not comparable; however, they do suggest the range in which the radius of tendon curvature must fall.

Table 5-2 presents data from the smallest subject hand (3 percentile female) and the largest subject hand (80 percentile male). The tendon-joint displacement radius of curvature values are given, and the force loadings on the tendons were predicted using equation 2.2. It can quickly be seen that this load almost doubled between the two subjects for the FDP tendons when the wrist is flexed. The FDS tendon results show the same effect during flexion, yet during extention the FDP and FDS tendons show more comparable force loading between the two subject hands.

An extrapolation to fifth and ninety-fifth percentile male and female tendon force loadings are given in Table 5.2.5. as radius of curvature value from equation 2.2. This equation is reasonable to use

as shown by Figure 5-1. The predicted r values from equation 2.2 correlate well (r^2= > .82 except hand 2) with the observed values from the four hands used in this report. Again, the trend to higher force loading on the tendon is seen as the wrist thickness decreases. The predicted values from Armstrong and Chaffin (1977), however, do not change with wrist anthropometry as dramatically as the observed values in Table 5-2. The load values predicted from observed data double between 3 percentile female and 80 percentile male in flexed wrist, while load values predicted from calculated tendon geometry increase only about twenty percent between 5 percentile female and 95 percentile male wrists in the flexed position.

The increase in force loading as wrist size decreases has implications on the environment to which the median nerve is subject in the carpal tunnel in the wrist. For example, the ischemic conditions described by Sunderland (1976) may be a product of direct impingement of the flexor tendons on the median nerve and the surrounding blood vessels. The load on those tendons is then an indicator of the degree of the impingement. Results shown in Table 5-2 and Table 5-2a give an indication of the environment around the median nerve. Larger force loading in smaller wrists may imply greater susceptibility to median nerve ischemia and CTS symptoms.

As reported by Armstrong (1975), the FDS tendons tend to have a larger radius of curvature value than the FDP tendons during extension and flexion as given by the tendon-joint displacement measurements, yet there are deviations from this trend (Table 5-1). The tendon location data do not show any general relationships between FDS and FDP tendons during extension or flexion.

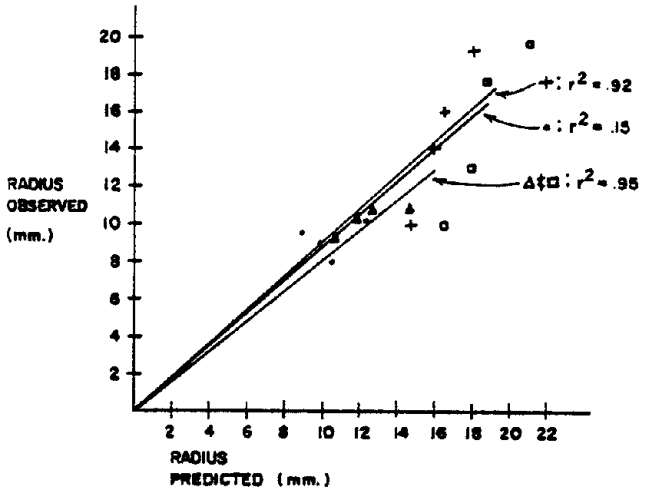

TYPE	SYM.	REG. COEF	r^2	STD. ERROR (mm.)
FDS EXT.	Δ	.82	.95	.83
FDP EXT.	●	.89	.15	1.1
FDS. FLX.	□	.82	.86	3.0
FDP FLX.	+	.92	.96	2.8

Figure 5-1: Observed Radius of Curvature from Equation 2.2 vs. Predicted Radius of Curvature from Equation 4.1.

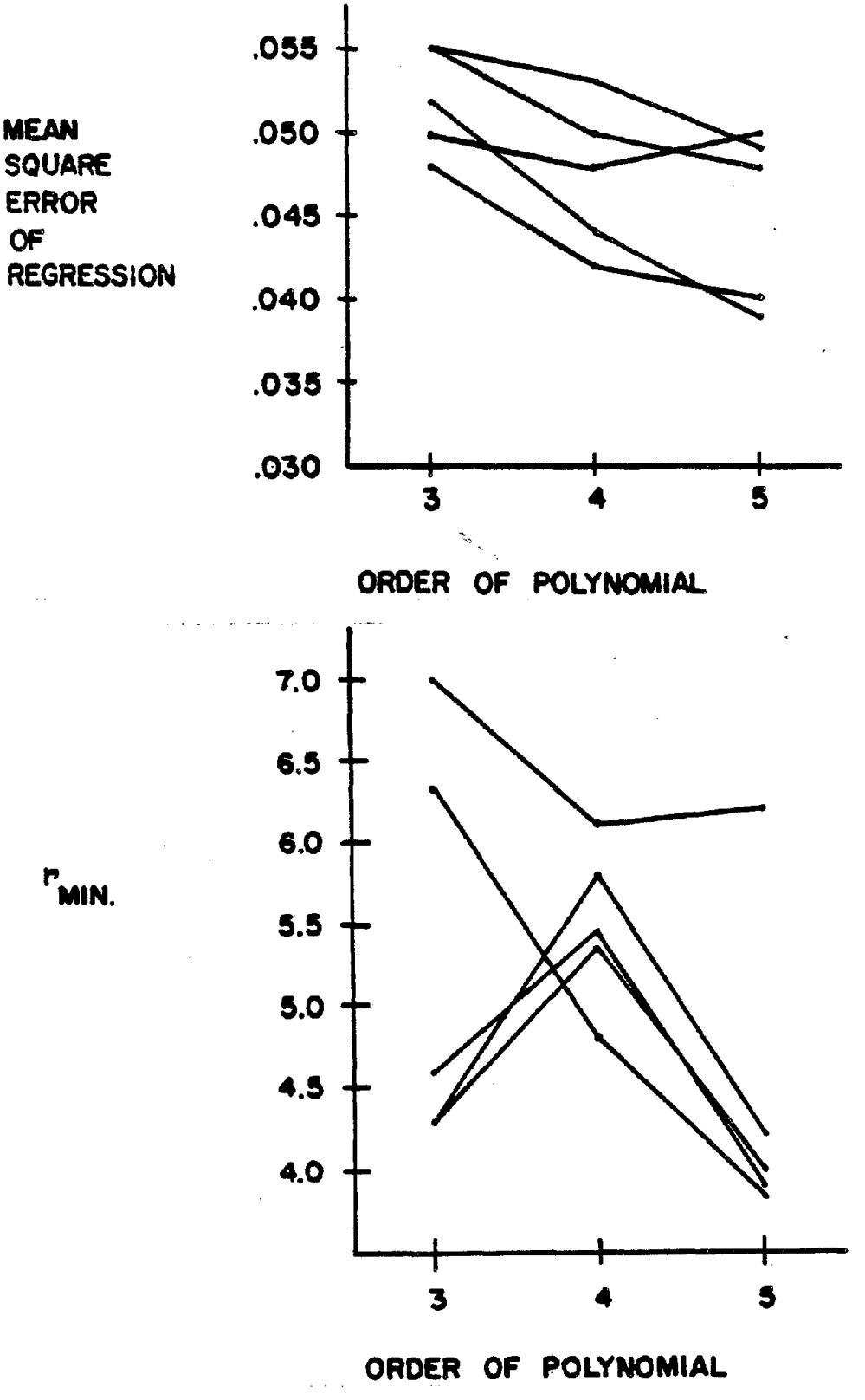

Figure 5-2: Effects of Increasing Order of Polynomial on Regression Error and Radius of Curvature Fit to Selected Tendon Location Data of Hand 4 in the Flexed Position

Table 5-1: Summary of Average Radius of Curvature Values for 3 Methods of Approximation in Cm.

		Extended		Flexed	
	Type	FDS	FDP	FDS	FDP
Hand 1	Displacement	1.02	.90	1.29	1.41
	Location Polynomial	3.42	3.68	11.0	5.1
	Location Splines	2.54	3.12	8.20	5.0
Hand 2	T - J Disp.	1.04	.88	1.74	1.59
	Location Polynomial	2.37	2.76	4.38	6.52
	Location Splines	3.00	2.55	4.04	3.49
Hand 3	T -J Displ.	1.10	.99	1.94	1.95
	Location Polynomial	3.19	2.75	2.75	4.36
	Location Splines	2.85	3.09	3.39	3.82
Hand 4	T - J Displ.	.95	.96	1.00	.98
	Location Polynomial	4.54	3.13	3.74	1.96
	Location Splines	2.94	3.35	3.14	4.10

Table 5-2: Radius of Curvature and Resulting Calculated Load on Tendon from Eq. 2.2

		Extended		Flexed	
		FDS	FDP	FDS	FDP
Hand 4	T - J Displ - R (Cm.)	.95	.96	1.00	.98
	Load (Flar Leng.) (K Pond)	1.05	1.04	1.00	1.11
Hand 3	T - J (Cm.) Displ - R	1.10	.99	1.94	1.95
	Load (K Pond)	.91	1.01	.52	.51
Percentile Male	Load (Kilopond/ ARC Length) = F_t/R F_t = 1 Kilopond				

Table 5-2-5: Radius of Curvature from Equation 4-1 and Resulting Calculated Load on Tendon from Equation 2-2

	(Cm.*) Wrist Thick-ness		Extended		Flexed	
			FDS	FDP	FDS	FDP
Percentile Female	3.18	(cm)	1.07	.89	1.68	1.50
		Load Kp/ARC leng.	.93	1.12	.60	.67
Percentile Female	3.43		1.14	.95	1.74	1.56
		Load	.88	1.05	.57	.64
Percentile Male	3.55	Placement	1.18	.98	1.78	1.59
		Load	.85	1.02	.50	.63
95% Male	4.48	Kan	1.44	1.20	2.05	1.81
		K plarc Leng. Load	.69	.83	.49	.55

* Wrist Thickness Estimated from Garrett (1970) Using Formula for Cir. of Ellipse.

Figure 4-1 shows the location of the resulting minimum radius of curvature values as given by the splines method of polynomial curve fitting. The minimum radius of curvature for the flexor tendons during wrist extension was found to be in a more distal portion, distal to the flexor retinaculum of the carpal tunnel than during wrist flexion at the distal edge of the flexor retinaculum. As demonstrated above, small radii of curvature imply high force loadings on the tendon and induce an environment which may contribute to ischemia of the median nerve and median nerve lesions.

The results showing the location of the minimum radius of curvature then correlate with results by Tanzer (1959) and Smith, et al., (1977), who showed that compressive force was higher in the distal portion of the carpal tunnel during wrist extension and in the proximal portion during wrist extension and flexion.

Both the tendon-joint displacement data and the tendon location data indicate a smaller radius of curvature during extension than during flexion, which agrees with data from Armstrong (1975). The splines method of fitting polynomials to the data generally gave a smaller radius of curvature for a given tendon than direct polynomial fitting with comparable error (Table 4-6). The resulting radius of curvature and error of regression generally decreased as the order of the polynomial increased (Figure 5-2). This result might be expected due to the greater degrees of freedom of the higher order polynomial.

5.2 WRIST SIZE CONTRIBUTION TO CTS

The results in Table 4-13 show the mean results for five measurements of wrist bone structure as described in section 3.2. When the pooled control and CTS data are compared for the five measurements with a paired t-test, no significant difference is found in any of the measurements between the two sample population. Only carpal angle is shown to be statistically significant ($p<.05$). This result indicates that observation of bone structure as seen in a radiograph in terms of gross size differences may not be indicative of a predisposition to CTS. These bone sizes were originally chosen to represent a direct indication of carpal tunnel volume. Therefore, changes in these bone structures should indicate a change in carpal tunnel volume. By comparing bone structures of CTS subjects and non-CTS subjects, an attempt was made to relate the occurrence of CTS to carpal tunnel volume. Again, the results showed no relationship from the measurements used. This method did not show any significant differences between CTS and non-CTS for a population of a single gender, but may show differences between male and female populations.

5.3 PREDICTIVE MODELS FOR HAND LINK LENGTHS

Tables 4-14 through 4-17 present five models for the prediction of link length from bone length for the distal, middle, and proximal phalanges and the metacarpals respectively. Model II seems to give the best results for the distal phalange and the metacarpals as

indicated by the standard error of regression. Model IV gave a similar error for these phalanges and the metacarpals. Model II tested only for differences in intercepts among the simple linear regression models for the five digits. Model IV tested for differences in both slope and intercept among the simple linear regression models for the five digits. Model IV gave the best results for the middle phalanges according to the standard error of regression. Model IV tests for differences in both slope and intercept among the simple linear regression models for the five digits fitting the resulting line through the origin. Models III and V gave best results for the proximal phalange. Model V performs the same analysis as Model IV without restricting the constant term to zero. These models may be used in constructing biomechanical simulations of the hand as well as predicting the capabilities of disabled and handicapped workers in the occupational environment.

VI. SUMMARY AND CONCLUSIONS

6.1 SUMMARY

Carpal Tunnel Syndrome results from compression of the median nerve in the carpal tunnel. The compression may be caused by anything which increases the pressure in the carpal tunnel or by direct impingement of the finger flexor tendons on the nerve. CTS may occur in the industrial environment due to repeated hand motions and especially when high forces are required of the hand.

This report has shown that the radius of curvature of the finger flexor tendons may range from about .9 centimeters to 4.0 centimeters and the radius of curvature is larger during flexion than extension. A smaller radius of curvature implies higher force loadings on the tendon during extension and flexion of the wrist joint. This report has also shown that five bone dimensions which indicate wrist size and hand length do not indicate a predisposal of the wrist to CTS.

Included in this report was a predictive model of link length from bone length for the phalanges and metacarpals of the hand. Several multivariate regression models were tested, and the models which minimized the standard error of regression were chosen as representative of predictors of link length.

6.2 CONCLUSIONS AND RECOMMENDATIONS

6.2.1 CONCLUSIONS

Through the experimentation and results discussed in this report, the original hypothesis that intra-wrist forces on the tendon increase significantly as joint thickness decreases has been shown to be true

for the tendons during wrist flexion, but not for wrist extension. The hypothesis that variations in wrist structure, as indicated by five chosen dimensions, are an etiological factor in the occurrence of CTS has been shown to be false. No significant difference was found between wrist bone measurements of normal control and CTS subjects, except in the carpal angle.

6.2.2 RECOMMENDATIONS FOR FURTHER STUDY

Further cadaver study should be done to determine if the values obtained for radius of curvature may be replicated. In creating a larger data base from the cadaver study, perhaps a reliable model of tendon geometry may be developed. Also, a thorough study should be done to define the characteristics of the splines method of approximating tendon radius of curvature with the present data. The radiographs which are available may be put to further use by studying other dimensions of the wrist and hand in an attempt to relate wrist bone structure to CTS.

REFERENCES

Armstrong, T.J. and Humes, R. An Experimental Investigation of the Relationship Between the Positions of the Hand and the Lengths of the Extrinsic Finger Flexor Muscles. Technical Report, Department of Industrial and Operations Engineering, The University of Michigan, 1975.

Barenco, S. and Strelka, E. "Carpal Tunnel Syndrome." Virginia Medical Monthly 103:122-124, February, 1976.

Barnes, C.G. and Currey, H.L.F. "Carpal Tunnel Syndrome in Rheumatoid Arthritis. A Clinical and Electrodiagnostic Survey." Ann. Rheum. Dis., 26;226-233, 1967.

Brain, W.R.; Wright, A.D. and Wilkinson, M. "Spontaneous Compression of Both Median Nerves in Carpal Tunnel." Lancet, 1:227-282, March 1947.

Cailliet, R. Hand Pain and Impairment. (Philadelphia: F.A. Davis, Co.), 1975, Second Edition.

Curtis, R.M. and Eversmann, W.W. "Internal Neurolysis as an Adjunct to the Treatment of the Carpal-Tunnel Syndrome." J. of Bone and Joint Surgery, 55-A(4):733-740, June 1973.

Eversmann, W. and Ritsick, J. "Intraoperative Changes in Motor Nerve Conduction Latency in Carpal Tunnel Syndrome." The Journal of Hand Surgery 3:77-81, January, 1978.

Gainer, J. and Nuggent, G. "Carpal Tunnel Syndrome: Report of 430 Operations" Southern Medical Journal, 70:325-328, March 1977.

Garrett, J.W. "Anthropometry of the Hands of Male Air Force Flight Personnel." Aerospace Medical Research Laboratory, Aerospace Medical Division, Air Force Systems Command, Wright-Patterson Air Force Base, Ohio, March, 1970.

Garrett, J.W. "Anthropometry of the Air Force Female Hand." Aerospace Medical Research Laboratory, Aerospace Medical Division, Air Force Systems Command, Wright-Patterson Air Force Base, Ohio, March, 1970.

Gray, R.N. Attorney's Textbook of Medicine, Vol. 1 & 4, (New York: Matthew Bender and Company), 1969.

Harper, H.; Poznanski, A.; Garn, S. "The Carpal Angle in American Populations." Investigative Radiology 9:217-221, July - August, 1974.

Herbison, G.J.; Teng, C.; Martin, J.H. and Ditunno, J.F., Jr. "Carpal Tunnel Syndrome in Rheumatoid Arthritis." Amer. J. of Phys. Med., 52;68-74, 1973.

Hymovich, L. and Lindholm, M. "Hand, Wrist, and Forearm Injuries." J. of Occup. Med., 8(11), November, 1966.

Kendall, David "Non-Penetrating Injuries of the Median Nerve at the Wrist." Brain, 73:84, 1950.

Kemble, F. "Electrodiagnosis of the Carpal Tunnel Syndrome." J. Neurol. Neurosurg. Psychiat., 31:32-27, 1968.

Landsmeer, J.M.F. "Studies in the Anatomy of Articulation." Acta Morphologica Neerlands Scandinavica, Vol. 3-4, 1960-62.

Leveau, B. Biomechanics of Human Motion. (Philadelphia: W.B. Saunders, Co., 2nd ed.), 1977.

Mohr, E. "An Investigation of Job Work Methods as Etiological Factors of Carpal Tunnel Syndrome." Occupational Health and Safety Technical Report, Department of Industrial Engineering, The University of Michigan, 1977.

Nicholas, G.; Noone, R.; Graham, W. "Carpal Tunnel Syndrome in Pregnancy." Hand 3:80, 1971.

Phalen, G.S. "The Carpal Tunnel Syndrome." Clinical Orthopaedics and Related Research. No. 83:29-40, March-April, 1972.

Phalen, G.S. "The Carpal Tunnel Syndrome." J. Bone and Joint Surgery, 48-A(2):211-228, March 1966.

Plaja, J. "Comparative Value of the Different Electrodiagnostic Methods in the Carpal Tunnel Syndrome." Scandinavian Journal of Rehabilitation Medicine, 3:101-108, 1971.

Pofnanski, A. The Hand in Radiologic Diagnosis, (Philadelphia: Saunder Co.) 1974.

Rabourn, R.A. Investigation of Individual Work Methods as Etiological Factors of Carpal Tunnel Syndrome. Technical Report, Department of Industrial and Operations Engineering, The University of Michigan, 1977.

Smith, E.M.; Sonstegard, D.A. and Anderson, W.H. "Contribution of Flexor Tendons to the Carpal Tunnel Syndrome." Archives of Phys. Med. and Rehab., (1976).

Tanzer, R.C. "The Carpal-Tunnel Syndrome." J. of Bone and Joint Surgery. 41-A(4):626-634, June 1959.

Tichauer, E.R. "Some Aspects of Stress on Forearm and Hand in Industry." JOM, 8(2):63:71, February, 1966.

Ulrich, L. "Anatomical Variations of the Median Nerve in the Carpal Tunnel." Journal of Hand Surgery 2:44-53, January, 1977.

Welch, R. "The Causes of Tenosynovitis in Industry." Industrial Medicine, 41(10):16-19, October 1972.

:PORT DOCUMENTATION PAGE	1. REPORT NO.	2. PB8	3. Recipient's Accession No. 8 247705/AS
Title and Subtitle Biomechanical Analysis of Personal CTS Attributes			5. Report Date 78/04/21
			6.
Author(s) Rolecki, J. M.			8. Performing Organization Rept. No.
Performing Organization Name and Address partment of Industrial and Operations Engineering, University Michigan, Ann Arbor, Michigan			10. Project/Task/Work Unit No. 11. Contract(C) or Grant(G) No. (C) (G) OH-00161-05
Sponsoring Organization Name and Address			13. Type of Report & Period Covered 14.

Supplementary Notes

Abstract (Limit: 200 words)

he importance of wrist size and the effect of high force loads on tendons were vestigated in relation to carpal tunnel syndrome (CTS). The geometry of the curvature the finger flexor tendons as they pass over the trochlea of the wrist was estimated ing a relationship between the change in joint angle of the wrist and displacement of e flexor tendon to determine the radius of curvature of the tendon. Human cadaver limbs re dissected and direct measurement were made of the spatial location of the tendon. e radius of curvature of the tendon in the vicinity of the trochlea was determined by tting polynomials to the data. The radius of curvature of the finger flexor tendons was und to range from about 0.9 to 4.0 centimeters. The radius of curvature was larger ring flexion than extension. Higher force loadings on the tendon during extension and exion of the wrist joint may be implied by a smaller radius of curvature. No edisposition of the wrist to the development of CTS was evidenced by the five bone mensions which indicate wrist size and hand length. Intra wrist forces on the tendon creased significantly as joint thickness decreased during wrist flexion, but not during tension. Variations in wrist structure were not found to be an etiological factor in e occurrence of CTS. The authors recommend that further cadaver study be done to termine whether the values for radius of curvature can be replicated.

Document Analysis a. Descriptors

b. Identifiers/Open-Ended Terms

[OSH-Publication, NIOSH-Grant, Grant-Number-OH-00161-05, sculoskeletal-system-disorders, Skeletal-system-disorders, Hand-injuries, Arm-injuries, omechanics, Ergonomics

c. COSATI Field/Group

Availability Statement	19. Security Class (This Report)	21. No. of Pages
	20. Security Class (This Page)	22. Price PB 149 856.93

ANSI 239.18) See Instructions on Reverse OPTIONAL FORM 272 (4-77)